

N O T I C E

THIS DOCUMENT HAS BEEN REPRODUCED FROM
MICROFICHE. ALTHOUGH IT IS RECOGNIZED THAT
CERTAIN PORTIONS ARE ILLEGIBLE, IT IS BEING RELEASED
IN THE INTEREST OF MAKING AVAILABLE AS MUCH
INFORMATION AS POSSIBLE

BWg 16 E-17



Technical Memorandum 83825

(NASA-TM-83825) INFORMATION THEORY LATERAL
DENSITY DISTRIBUTION FOR EARTH INFERRED FROM
GLOBAL GRAVITY FIELD (NASA) 64 P
HC A04/MF A01

N82-19731

CSCL 08N

Unclass

G3/46 16369

Information Theory Lateral Density Distribution for Earth Inferred from Global Gravity Field

David Parry Rubincam

OCTOBER 1981

National Aeronautics and
Space Administration

Goddard Space Flight Center
Greenbelt, Maryland 20771



**INFORMATION THEORY LATERAL DENSITY
DISTRIBUTION FOR EARTH INFERRED
FROM GLOBAL GRAVITY FIELD**

David Parry Rubincam

**Geodynamics Branch, Code 921
Goddard Space Flight Center
Greenbelt, MD 20771**

ABSTRACT

Information Theory Inference, better known as the Maximum Entropy Method, is used to infer the lateral density distribution inside the earth. The approach assumes that the earth consists of indistinguishable Maxwell-Boltzmann particles populating infinitesimal volume elements, and follows the standard methods of statistical mechanics (maximizing the entropy function). The GEM 10B spherical harmonic gravity field coefficients, complete to degree and order 36, are used as constraints on the lateral density distribution. The spherically symmetric part of the density distribution is assumed to be known. The lateral density variation is assumed to be small compared to the spherically symmetric part. The resulting information theory density distribution for the cases of no crust removed, 30 km of compensated crust removed, and 30 km of uncompensated crust removed all give broad density anomalies extending deep into the mantle, but with the density contrasts being the greatest towards the surface (typically $\pm 0.004 \text{ g cm}^{-3}$ in the first two cases and $\pm 0.04 \text{ g cm}^{-3}$ in the third). None of the density distributions resemble classical organized convection cells. The information theory approach may have use in choosing Standard Earth Models, but, the inclusion of seismic data into the approach appears difficult.

PRECEDING PAGE BLANK NOT FILMED

INFORMATION THEORY LATERAL DENSITY DISTRIBUTION FOR EARTH INFERRED FROM GLOBAL GRAVITY FIELD

INTRODUCTION

The problem addressed here is inferring via information theory the lateral density variation inside the earth from the observed external anomalous gravity field. Information theory is used because it is the least subjective way to deal with inverse problems (Baierlein, 1971). The motivation for this study is the relationship of the lateral density variation to tectonics and convection.

The nature of the problem is the following. The lateral density variation inside the earth generates the observed gravity anomalies. Hence information about the lateral density variation is provided by examining the anomalies. However, the observed gravity anomalies cannot be inverted to recover the actual density variation. The problem is nonunique: there are an infinite number of density distributions which can generate the observed gravity field. This is unfortunate, since it is desirable to know the lateral density variation, especially with regard as to how it relates to tectonics and convection (Phillips and Lambeck, 1980).

The nonuniqueness can be dealt with by various approaches in order to obtain insight into the physics of the earth. Of these modeling is by far the most common approach. Here extra assumptions are introduced until the solution to the problem becomes unique. Kaula (1963), for instance, assumes that the shear strain energy of the mantle is minimized. This key assumption, and other minor ones, together with the constraints of the observed gravity field determine a unique lateral density variation. Phillips and Lambeck (1981) review many papers which use modeling. Another approach is the Backus-Gilbert method (Backus and Gilbert, 1967, 1968; Parker, 1977), which studies all possible solutions consistent with the given data. This study is called the geophysical inverse problem (Backus and Gilbert, 1967, p. 249). The Backus-Gilbert method has been used

extensively in seismology (e.g., Jordan and Franklin, 1971). Burkhard and Jackson (1976) apply the method to gravity data. There are also other approaches to data inversion; see, e.g., Parker (1977), Sabatier (1977), and references contained therein.

The approach to the lateral density variation used here is that of information theory (Jaynes, 1957, 1963, 1967). This approach is commonly known as the Maximum Entropy Method, or MEM for short. A better name would be Information Theory Inference (ITI for short), since information theory is its basis and the name avoids confusion with thermodynamic entropy (Baierlein, 1971, pp. 473-478). It will be called ITI here.

ITI is a probabilistic approach to nonuniqueness. Each possible answer (labelled i) to a non-unique problem is assigned a probability P_i that it is the correct answer. The probabilities P_i are assigned numerical values so as to maximize Shannon's (1948) information measure

$$MI = - \sum_i P_i \ln P_i \quad (1)$$

subject to the constraints of the known data. MI in (1) stands for "Missing Information," i.e., the amount of information needed to determine which answer is correct (Baierlein, 1971, p. 64). In practice the expectation value of the desired unknown quantity is taken as the inferred answer to the problem. The information theory approach thus provides a solution to what will be called the geophysical inference problem: picking one answer out of a number of possible answers as the most likely to be true. ITI may hence be regarded as a complementary method to the Backus-Gilbert method (Gull and Daniell, 1978), which investigates the geophysical inverse problem. The rationale for using ITI is that it picks the "best" answer, dictated by the information at hand, out of the many possible answers. "Best" here means "least subjective," i.e. the number of unconscious assumptions in choosing an answer is minimized (Tribus and Rossi, 1973). See Baierlein (1971, pp. 11-89) for an excellent introduction to ITI.

ITI (or MEM) has been used with great success in several different fields. One is statistical mechanics (Jaynes, 1957; Tribus, 1961; Katz, 1967; and Baierlein, 1971). In fact, (1) is the entropy function of statistical mechanics. The only difference between ITI and statistical mechanics lies in ITI's powerful information theory foundation, which allows the approach to be applied to a wide variety of problems, and not just to statistical mechanics. It has been so applied to spectral analysis (Burg, 1967, 1968, 1972) and to radio brightness maps of the sky (Gull and Daniell, 1978). In solid earth geophysics ITI has been applied to the spectral analysis of polar motion (e.g., Smylie et al., 1973; Graber, 1976), and to the radial density distribution of the earth (Rietsch, 1977; Rubincam, 1978, 1979; Graber, 1977) and of the planets (Koyama, 1979).

The present work is an extension of Rubincam (1979) to the lateral density variation. ITI is used to infer the lateral density structure based on the spherical harmonic coefficients of the gravity field and on an assumed spherically symmetric density distribution (also called the radial density distribution). The gravity field coefficients are those of GEM 10B (Lerch et al., 1981), complete to degree and order 36. The hydrostatic equilibrium bulge is subtracted out of the $\ell = 2, 4$, $m = 0$ terms using the hydrostatic coefficients of Nakiboglu (1979). Also subtracted from the GEM 10B terms when the need arises are the gravity field coefficients of a crustal model. Two different crustal models are used: one a 30 km-thick isostatically compensated crust and the other an isostatically uncompensated crust, also 30 km thick. Carl Wagner supplied the spherical harmonic coefficients for these models (Wagner, private communication, 1976). Both sets of coefficients are complete to degree and order 36. The radial density distribution is the average structure Parametric Earth Model (PEM) of Dziewonski et al., (1975). Further, the earth is assumed to be a sphere and that the lateral density variation is small compared to the radial density distribution.

The principal results are as follows. The information theory density distribution can be written as a spherical harmonic expansion. The equation for the density variation is similar in form

to that of the equation which gives density contrasts due to lateral temperature differences. For the cases where no crust or the 30 km thick compensated crust is removed the density contrasts are greatest near the earth's surface and have typical magnitudes of $\pm 0.004 \text{ g cm}^{-3}$. The density contrasts are also greatest near the surface for the case of 30 km of uncompensated crust removed and are typically a factor of 10 larger than in the two other cases. In all three cases the density contrasts decrease with depth but significant density anomalies still extend deep into the mantle. None of the three density distributions look like classical convection patterns, i.e., organized cells with columns of low density where material is rising and columns of high density where material is sinking. No attempt has been made in any of the cases to compute stresses or stress-differences.

DERIVATION OF THE INFORMATION THEORY DENSITY DISTRIBUTION

The information theory density distribution is derived from the following considerations. It is first assumed that the data consist of the known values F_q for Q integrals of the form

$$F_q = \int_V \rho(\vec{r}) f_q(\vec{r}) dv, (q=1, 2, \dots, Q), \quad (2)$$

where $\rho(\vec{r})$ is the earth's density distribution, $f_q(\vec{r})$ is a function which depends on position \vec{r} inside the earth, dv is a volume element, and V is the volume of the earth. Examples of integrals of this form are the mass and moment of inertia of the earth. The gravity field coefficients also have this form, since they can be written (Phillips and Lambeck, 1980, p. 30)

$$\bar{C}_{\ell m i} = \frac{\int_V \rho(\vec{r}) r^\ell \bar{Y}_{\ell m i}(\theta, \lambda) dv}{(2\ell+1) M_E a_E^\ell} \quad (3)$$

where $\bar{C}_{\ell m 1} = \bar{C}_{\ell m}$ and $\bar{C}_{\ell m 2} = \bar{S}_{\ell m}$ are the normalized coefficients of degree ℓ and order m , $r = |\vec{r}|$, and the $\bar{Y}_{\ell m i}(\theta, \lambda)$ are surface spherical harmonics using Kaula's (1967) 4π normalization,

with θ being colatitude and λ longitude. M_E and a_E are the mass and radius of the earth, respectively. Obviously in this case $F_q = \bar{C}_{\ell m i}$ and

$$f_q(\vec{r}) = \frac{r^\ell Y_{\ell m i}(\theta, \lambda)}{(2\ell+1) M_E a_E^\ell} \quad (4)$$

The next consideration in using ITI is to set up the earth models which constitute the various possible answers to the problem. The task is then to choose the "best" model based on the data of the form (2). The earth models are set up as follows: the earth is divided up into infinitesimal cubes, all with equal volume $dv = dx dy dz$. Each cube is labelled with the running subscript j . The position vector from the center of the earth to the j th cube is \vec{r}_j . The cubes are populated with indistinguishable particles of mass m . Each earth model i has n_{ji} particles in the j th cube where n_{ji} is an integer ≥ 0 . The density of the earth at position \vec{r}_j in the i th model is then $\rho_i(\vec{r}_j) = n_{ji} m / dv$. The integrals (2) for each earth model i become the sums

$$F_{qi} = \sum_j \left(\frac{n_{ji} m}{dv} \right) f_q(\vec{r}_j) dv = m \sum_j n_{ji} f_q(\vec{r}_j). \quad (5)$$

The expectation values

$$\langle F_q \rangle = \sum_i P_i F_{qi} \quad (6)$$

are assumed to constitute the observed values of F_q , where P_i is the probability that the i th model is in fact the correct model.

The problem so formulated is analogous to the standard statistical mechanics problem of determining the population numbers of indistinguishable particles following Bose-Einstein statistics using the grand canonical ensemble (Rubincam, 1979). (Indistinguishable particles are chosen since the interchanging of particles does not affect the density distribution, which is the topic under discussion.) The solution can thus be carried out in the usual statistical mechanics fashion

(Morse, 1969, pp. 316-319; Reif, 1965, pp. 346-349). (1) is maximized subject to the constraints of the data (6) and $\sum_i P_i = 1$:

$$\frac{\partial}{\partial P_i} \left[-\sum_i P_i \ln P_i + \alpha_0 \sum_i P_i + \alpha_1 \sum_i P_i F_{1i} + \dots + \alpha_Q \sum_i P_i F_{Qi} \right] = 0$$

where $\alpha_0, \dots, \alpha_Q$ are Lagrange multipliers, yielding $P_i = \exp(\sum_q \alpha_q F_{qi})/Z$, where

$$Z = e^{1-\alpha_0} = \sum_i \exp(\sum_q \alpha_q F_{qi}) \quad (7)$$

is the grand partition function. Using (5) in (7) gives

$$Z = \sum_i \exp \left[\alpha_1 \sum_j n_{ji} f_1(\vec{r}_j) + \dots + \alpha_Q \sum_j n_{ji} f_Q(\vec{r}_j) \right] \quad (8)$$

for Z , where $m\alpha_q$ has been redefined as α_q . Note that the partial derivative of the logarithm of (8) with respect to $\alpha_1 f_1(\vec{r}_j)$ gives

$$\begin{aligned} \frac{\partial \ln Z}{\partial (\alpha_1 f_1(\vec{r}_j))} &= \sum_i n_{ji} \exp \left[\alpha_1 \sum_j n_{ji} f_1(\vec{r}_j) + \dots + \alpha_Q \sum_j n_{ji} f_Q(\vec{r}_j) \right] \\ &= \sum_j n_{ji} P_i = \langle n_j \rangle \end{aligned} \quad (9)$$

which is the expectation value of the number of particles in the cube at position \vec{r}_j . This result will be used shortly.

If there are no limits to the number of particles occupying each cube, then (8) can be factored as (Morse, 1969, p. 326; Reif, 1965, p. 347)

$$Z = \prod_j Z_j$$

where

$$Z_j = \sum_{n_j=0}^{\infty} \exp \left\{ [\alpha_1 f_1(\vec{r}_j) + \dots + \alpha_Q f_Q(\vec{r}_j)] n_j \right\} \quad (10)$$

But this has the form $\sum_{n=0}^{\infty} x^n$, which is equal to $1/(1-x)$. Hence (10) becomes

$$Z_j = \frac{1}{1 - \exp [\alpha_1 f_1(\vec{r}_j) + \dots + \alpha_Q f_Q(\vec{r}_j)]} \quad (11)$$

Therefore

$$\langle n_j \rangle = \frac{1}{e^{-\alpha_1 f_1(\vec{r}_j) - \dots - \alpha_Q f_Q(\vec{r}_j)} - 1} \quad (12)$$

by (9). If it is now assumed that $\langle n_j \rangle \ll 1$, so that the Bose-Einstein statistics pass over to Maxwell-Boltzmann statistics (Reif, 1965, p. 352; Morse, 1969, p. 329), then the exponential term in the denominator of (12) is much greater than 1, and (12) simplifies to

$$\langle n_j \rangle \approx e^{\alpha_1 f_1(\vec{r}_j) + \dots + \alpha_Q f_Q(\vec{r}_j)}$$

Multiplying this by m/dv and dropping the subscript j gives the expression

$$\rho_1(\vec{r}) = \frac{m}{dv} \langle n_j \rangle = \frac{m}{dv} e^{\alpha_1 f_1(\vec{r}) + \dots + \alpha_Q f_Q(\vec{r})} \quad (13)$$

as the information theory density distribution. This is a most important result: it gives the form of the information theory density distribution for particles following Maxwell-Boltzmann statistics where the constraints on the density distribution have the form (2). The variance of the distribution is discussed in Appendix A.

The m/dv appearing in (13) is a troublesome factor. No commitment has been made either to the value of m or dv ; and there seems to be no clear guidance on how to choose their values. As it turns out, this problem may be avoided by absorbing the factor into the spherically symmetric part of the density distribution, as shown next.

The task now is to simplify (13). This involves two assumptions: first, that $f_1(\vec{r})$ pertains solely to the spherically symmetric part of the density distribution (explained below); and second, that

$$|\alpha_2 f_2(\vec{r}) + \dots + \alpha_Q f_Q(\vec{r})| \ll 1$$

so that

$$e^{\alpha_2 f_2(\vec{r}) + \dots + \alpha_Q f_Q(\vec{r})} \cong 1 + \alpha_2 f_2(\vec{r}) + \dots + \alpha_Q f_Q(\vec{r})$$

where the $f_2(\vec{r}), \dots, f_Q(\vec{r})$ are the appropriate functions (4) for the gravity field (i.e. the anomalous density variation is small compared to the radial density.) With these two assumptions (13) becomes

$$\rho_1(\vec{r}) \cong \frac{m}{dv} e^{\alpha_1 f_1(\vec{r})} \left[1 + \sum_{\ell mi} \frac{\alpha_{\ell mi} r^\ell \bar{Y}_{\ell mi}(\theta, \lambda)}{(2\ell+1) M_E \alpha_E^\ell} \right]$$

which may be written

$$\rho_1(\vec{r}) \cong \rho_0(r) + \sum_{\ell mi} \frac{\alpha_{\ell mi} \rho_0(r) r^\ell \bar{Y}_{\ell mi}(\theta, \lambda)}{(2\ell+1) M_E \alpha_E^\ell} \quad (14)$$

where

$$\rho_0(r) = \frac{m}{dv} e^{\alpha_1 f_1(\vec{r})} \quad (15)$$

with $\rho_0(r)$ being the spherically symmetric part of $\rho(\vec{r})$ and where subscripts ℓmi have been substituted for subscript q . Obviously taking $f_1(\vec{r})$ to be

$$f_1(\vec{r}) = \frac{1}{\alpha_1} \ln [\rho_0(r) dv/m]$$

results in (15). This is artificial, to be sure; no value f_1 in (2) is known for the earth where $f_1(\vec{r})$ has the form given above. However, it has two advantages: the troublesome factor m/dv disappears, and any desired $\rho_0(r)$ can be used in (14). The $\rho_0(r)$ for the earth is known to a high degree of accuracy from other data: it cannot differ greatly from the PEM $\rho_0(r)$ of Dziewonski et al., (1975). Hence it will be assumed here that the integral F_1 is known for the earth where $f_1(\vec{r})$ is given by the above equation, in order to use Dziewonski et al.'s (1975) radial density distribution.

All that remains to find the information theory density distribution is to evaluate the $\alpha_{\ell m i}$ using the gravity field coefficients. The raw gravity field coefficients given by (2) will not be used, however, for two reasons. The first reason is that the contribution of the earth's hydrostatic equilibrium rotational bulge to the gravity field must be subtracted out. The second reason is that the gravity field of the crust must also be subtracted from the coefficients when a crustal model is used. In this case the gravity field data become

$$\hat{C}_{\ell 0 1} = \bar{C}_{\ell 0 1}^{\text{GEM}} - \bar{C}_{\ell 0 1}^{\text{CR}} - \bar{C}_{\ell 0 1}^{\text{HE}}$$

for the $\ell = \text{even}$, $m = 0$, $i = 1$ terms and

$$\hat{C}_{\ell m i} = \bar{C}_{\ell m i}^{\text{GEM}} - \bar{C}_{\ell m i}^{\text{CR}}$$

for the other coefficients. The superscripts GEM, HE, and CR stand for "Goddard Earth Model," "Hydrostatic Equilibrium," and "Crust" respectively. Actually only the $\ell = 2$ and $\ell = 4$ hydrostatic equilibrium coefficients computed by Nakiboglu (1979) for Dziewonski et al.'s (1975) PEM will be used here; the higher degree hydrostatic equilibrium terms are assumed to be zero. Strictly, these terms should be included, but their computation is difficult and the error in ignoring them is probably small. All of the crustal terms up to and including degree and order 36 will, however, be subtracted from the GEM 10B coefficients when a crustal model is used.

Substituting (14) for $\rho(\vec{r})$ and $\hat{C}_{\ell mi}$ for $\bar{C}_{\ell mi}$ into (2) to evaluate the $\alpha_{\ell mi}$ yields

$$\rho_I(\vec{R}) = \rho_0(R) \left[1 + \sum_{\ell mi} \delta_{\ell} \hat{C}_{\ell mi} R^{\ell} \bar{Y}_{\ell mi}(\theta, \lambda) \right] \quad (16)$$

as the information theory density distribution, where the

$$\delta_{\ell} = \frac{(2\ell+1) \bar{\rho}_E}{3 \int_0^{R_U} \rho_0(R) R^{2\ell+2} dR} \quad (17)$$

are found by using the orthogonality properties of the $\bar{Y}_{\ell mi}(\theta, \lambda)$, where the earth is assumed to be a sphere, and where the variable r has been replaced by $R = r/\bar{a}_E$ for convenience so that $0 \leq R \leq 1$. Also, $\bar{\rho}_E$ is the average density of the earth and $\bar{a}_E = 6371$ km is the radius of the earth. R_U is the radius of the sphere in which the unknown density distribution to be inferred resides (the subscript u standing for "Upper.") For example, $R_U = 1$ if no crust is stripped off the earth and $R_U = 6341/6371$ if a 30 km thick crust is stripped off. The integral in the denominator of (17) can be evaluated analytically, since Dziewonski et al. (1975) break up the earth into eight shells, with $\rho_0(R)$ being given as a polynomial in R in each shell. Table 1 gives the δ_{ℓ} resulting from this computation for $R_U = 1$ and for $R_U = 6341/6371$.

RESULTS AND COMPARISONS WITH OTHER STUDIES

The fundamental equations of this paper are (16) and (17). What they give is, in a sense, the broadest possible density anomalies; more localized anomalies are not warranted by the data. Some general features of these equations should be noted before examining specific density distributions.

The information theory density distribution $\rho_I(\vec{r})$ (the subscript I standing for "Information Theory") given by (16) is obviously a spherical harmonic expansion of the form

$$\rho_I(\vec{R}) = \rho_0(R) + \Delta\rho_I = \rho_0(R) + \sum_{\ell mi} \bar{\rho}_{\ell mi}(R) \bar{Y}_{\ell mi}(\theta, \lambda) \quad (18)$$

where

$$\Delta\rho_l = \sum_{\ell m l} \bar{\rho}_{\ell m l}(R) \bar{Y}_{\ell m l}(\theta, \lambda), \quad \bar{\rho}_{\ell m l}(R) = \delta_\ell C_{\ell m l} R^\ell \rho_0(R). \quad (19)$$

Note that $\Delta\rho_l$ changes discontinuously when $\rho_0(R)$ does. Also, (16) has a form similar to that of the equation giving a density variation due to lateral temperature differences (e.g. Phillips and Lambeck, 1980, p. 32):

$$\rho = \rho_0 [1 - \alpha(T - T_0)] \quad (20)$$

Here α is the coefficient of thermal expansion, ρ_0 and T_0 are the reference density and reference temperature, respectively, while T is the temperature. (The reason (16) has this form is due to the assumption that $\Delta\rho_l$ is small compared to $\rho_0(R)$). So (16) is consistent with the idea that the density anomalies are due to lateral temperature differences—but does not necessarily imply that the anomalies are so caused.

It should further be noted that there is no point in computing the power spectrum of the anomalous potential $V_\ell^2(\Delta U)$ (e.g. Phillips and Lambeck, 1980, equation 11) generated by the density distribution (16), since the field coefficients are the given data, which (16) automatically satisfy. Moreover, the information theory density distribution (16) does not have a white noise spectrum, which Lambeck (1976) (see also Phillips and Lambeck, 1980) found will reproduce the observed anomalous potential spectrum (i.e. Kaula's (1967) rule-of-thumb). Instead the information theory density distribution $\rho_l(\vec{R})$ concentrates the density anomalies towards the earth's surface, due to the R^ℓ behavior of $\bar{\rho}_{\ell m l}(R)$ and the ℓ^2 behavior of δ_ℓ in (19). (The ℓ^2 behavior may be seen by substituting $\bar{\rho}_E$ for $\rho_0(R)$ in (17) and evaluating the integral.) Also, it is clear from (19) that the lower degree anomalies are spread more evenly throughout the earth than the higher degree anomalies. This concentration of density anomalies towards the surface is in contrast to the findings of the Monte Carlo studies of Kaula (1977) and the mass-point studies of Lowrey (1978),

who indicate that the anomalies may increase with depth. Dziewonski et al. (1977) and Julian and Sengupta (1973), among others, also indicate that large anomalies are to be found deep within the mantle on the basis of seismic travel time studies. The statistical gravity study of Khan (1977), however, places most of the anomalies in the upper mantle. The seismic studies of Romanowicz (1979) and Cara (1979) and others show considerable upper mantle lateral structure, while the analysis of satellite-to-satellite tracking data by Marsh et al. (1981) indicates that most of the gravity anomalies in the Pacific can be explained by lithospheric sources.

It should be mentioned that the density anomalies given by (16) and (17) are not confined to the crust and mantle, but extend into the core as well. To exclude them from the core the lower limit of the integral in (17) would have to be replaced by R_L (the subscript L standing for "Lower"), where $R_L = 3485.7/6371.0$, the radius of the core being 3485.7 km. In practice excluding the density anomalies from the core makes little difference in the resulting density distribution for the crust and mantle. Finally, the boundaries where $\rho_0(R)$ changes discontinuously are assumed to be spherical, so that there is no possibility of density anomalies arising from bumps on these boundaries in the manner of Hide and Horai (1968) and McQueen and Stacey (1976), for example.

The above constitute the general remarks on the information theory density distribution. Specific examples are discussed next.

A computer program was written to produce maps in order to examine specific information theory density distributions.* All of the maps are based on the GEM 10B gravity field (Lerch et al., 1981). The GEM 10B field is based on satellite, surface gravity, and GEOS-3 altimetry data. Since GEM 10B is complete to degree and order 36, the limit of resolution is about 5 degrees of arc, or about 550 km on the earth's surface. All of the higher degree terms ($l \geq 16$) are assumed to be meaningful, although Phillips and Lambeck (1980, p. 44) warn that these terms may largely be noise.

*See Appendix B for a listing of the program.

Plate 1 shows the density variation $\Delta\rho_1$ given by (19) overlaid on the global tectonic and volcanic activity map of Lowman (1981). The density variation is given on the surface of a sphere with radius 6368.0 km. It is at this depth, 3 km, that the oceans leave off and the rock surface begins in Dziewonski et al.'s (1975) PFM. No crust has been stripped off. The interval between contour lines is 0.002 g cm^{-3} . This map looks quite similar to the GEM 10B free-air gravity anomaly map (S. Klosko, private communication, 1980). It shows such typical features as the lows at Hudson Bay, Fennoscandia and some of the abyssal plains (e.g., Somali, Hatteras); and highs at some slow-moving ocean ridges (e.g., Mid-Atlantic, Southwest Indian Ocean), subduction zones (e.g., Peru-Chile, Tonga-Kermadec), and hot spots (e.g., Hawaii, Iceland). Hence for qualitatively relating density and tectonics, similar to relating gravity to tectonics as done by Kaula (1972), a free-air gravity anomaly map might just as well be used.

The map shows regions of artificial densities, due to the assumption that the earth is a sphere; the topography has been flattened. So at the Mid-Atlantic Ridge south of Iceland, for example, the effect of topography more than cancels the effect of the low density material upwelling beneath the ridge (assuming the basic validity of plate tectonics), producing a positive anomaly (Lambeck, 1972) and hence an artificially high density.

Plate 2 shows the density distribution at 30 km depth ($r \approx 6341 \text{ km}$), where 30 km of isostatically uncompensated crust has been stripped off the earth (giving essentially the Bouguer anomalies). The interval between contour lines is 0.02 g cm^{-3} . Note that it gives low densities at some subduction zones. Removing the Andes, for example, completely erases the positive anomaly of Plate 1, so that low densities prevail. There is no sign of a high density subducting slab (which is probably too small to be seen in any case with the resolution employed here).

Figures 1, 2, and 3 show $\Delta\rho_1$ on a plane which slices through the center of the earth in the equatorial plane for the cases of no crust removed, 30 km of isostatically compensated crust removed, and 30 km of isostatically uncompensated crust removed, respectively. The equatorial plane was

chosen because it illustrates typical features of such slices, plus one atypical feature which appears in Figure 2.

All three figures illustrate a remark made earlier: that the information theory density anomalies extend deep into the earth, but the greatest density variation occurs near the surface. This is in qualitative agreement with Arkani-Hamed's (1970) minimum shear strain energy density distribution, but his density anomalies are much larger than those shown here. The figures also show regions where $\Delta\rho_1$ changes sign with depth. This is also in qualitative agreement with Sanchez's (1980) density distribution which minimizes the sum of the mantle shear strain energy plus gravitational potential energy. The size of the density variation shown in Figures 1 and 2 is in fair agreement with Sanchez (1980). However, the density distribution across Sanchez's (1980) slice through the equatorial plane looks nothing like those shown in the figures. It should be mentioned that the minimum energy solutions of Kaula (1963), Arkani-Hamed (1970), and Sanchez (1980) give nonhydrostatic stresses which probably exceed the finite strength of the mantle, indicating that the assumed elastic rheology is unrealistic (Lambeck, 1976, p. 6333). The alternation of the sign of $\Delta\rho_1$ with depth is also in qualitative agreement with Lewis and Dorman (1970), who used a communications theory approach to the relation of density to topography.

The information theory density distributions shown in Figures 1 to 3 clearly tend to form "pockets" of high and low density extending downwards from the surface. There is no obvious convection pattern shown in any of the figures. None of them show what look like classical convection cells; that is, organized columns of low density material moving upwards and columns of high density material moving downwards. Pockets which slant at an angle to the local normal (such as the low density region at 305 degrees east longitude shown in Figure 2, for example) look like they might indicate some sort of horizontal as well as vertical motion of material. But closer examination of the region around such features generally reveals that there are other pockets of similar density slanting towards them (as is obvious with the two low density pockets between 60

and 90 degrees east longitude shown in Figure 1, for example) which are not contoured. Hence the apparent "motion" is probably an artifact of the contouring process.

The one atypical feature mentioned earlier is the high density "blob" located at 285 degrees east longitude shown in Figure 2. Closer examination of this feature shows that it is a "tube" of high density material connecting the Peru-Chile Trench with the Middle America Trench. This feature is atypical in that the greatest density contrast occurs beneath the surface, while with the pockets the greatest density contrast occurs at the surface of the sphere inside which the density distribution is inferred.

Figures 1 and 2 are quite similar to each other. The reason for this is that the removal of a 30 km-thick isostatically compensated crust affects mostly the high degree spherical harmonic terms, and not the low degree terms considered here. The density distribution shown in Figure 3 is of course dominated by the removal of the uncompensated topography, and not the GEM 10B gravity field.

If the density anomalies of Figures 1 and 2 are assumed to be due to lateral temperature variation, then typical temperature differences of 100 K are required, assuming α in (20) is about $3 \times 10^{-5} \text{ K}^{-1}$ (e.g., Phillips and Lambeck, 1980, p. 53). The temperature differences must be about a factor of 10 greater to explain the density anomalies of Figure 3, assuming the same value for α .

Maps showing the density distribution with the degree of the gravity and crustal fields restricted to $\ell \leq 16$ also give pockets similar to those shown in the figures. Hence it appears that the qualitative behavior of the information theory density distribution will not change if terms of higher degree ($\ell > 36$) than those considered here are included in the fields.

DISCUSSION

One question which arises is which of the three density distributions considered here is to be preferred. Obviously the one in which no crust is removed is over-abstracted: no account is taken of the topography. So it is not the preferred density distribution. The density distribution in which 30 km of uncompensated crust is removed has intriguing consequences for the deep structure of continents (e.g., Jordan, 1975; but see Anderson, 1979): very deep indeed. However, the geo-physical evidence favors the density distribution in which 30 km of compensated crust is removed; so it is preferred. But it is not ideal: it assumes that the topography is isostatically supported everywhere over the earth; and, moreover, with a depth of compensation of 30 km. This is certainly not the case. To cite just one example where the assumptions fail, no account is taken of thermal isostasy at the ocean ridges (Haxby and Turcotte, 1978), where the effective depth of compensation is greater than 30 km. Hence the density distribution still gives a high density for the Mid-Atlantic Ridge south of Iceland, for example, after the crust is removed, when it should be low density. Hence better models of the crust are needed in order to use ITI to infer the density distribution below it.

Another question which arises is why the information theory density distribution disagrees with the results of Lambeck (1976), Kaula (1977), and Lowrey (1978) which are also based solely on the relationship of density to gravity (and not on seismic travel times), and which give large density anomalies in the lower mantle. The answer appears to be that these studies examine only a limited number of models which mimic the external gravity field, while the information theory density distribution is a weighted average over all possible density models and reproduces the external gravity field exactly.

The reason why the information theory density distribution disagrees with the seismic evidence of Julian and Sengupta (1973), Dziewonski et al. (1977) and others, which also give large anomalies in the lower mantle, seems clear enough: the seismic data have not been included in the information theory approach. Their inclusion presumably would show large anomalies in the lower mantle.

The dominant impression from the foregoing remarks on the problem addressed here is one of simplicity. More data must be introduced to obtain results which are closer to the actual state of affairs inside the earth. Taking the earth to be made up of indistinguishable particles following Maxwell-Boltzmann statistics is an obviously simplifying, if fundamental assumption which must also be dealt with in order to obtain more realistic results.

Introducing seismic travel times into the approach appears to be an obvious next step to take in examining the density anomalies. However, including the seismic travel time data into ITI appears to be difficult. It is not obvious how to put such information into an approach which sums over all possible models. Numerical models are out of the question: dividing up the earth into 10 volume elements each of which may be occupied by up to 10 particles gives 10^{10} models to consider -- far too many already for a computer. Thus the problem must be done analytically. But even such a seemingly simple task as using free oscillation periods to obtain a spherically symmetric earth model has analytical difficulties: the data do not have the simple form (2), and the elastic parameters vary as well as the density. These difficulties make the evaluation of the partition function Z troublesome (Graber, 1977). The variance (see Appendix A) and choosing m/dv in (13) also pose difficulties in applying ITI.

On the positive side is the heart of the method: ITI (MEM) minimizes subjectivity. To illustrate, there is no need in ITI to decide which lower degree harmonics to ignore in examining density anomalies in the lithosphere (e.g., Marsh et al., 1981), which is a highly subjective procedure. ITI weights all the harmonics automatically. And since ITI gives the one "best" (i.e., least subjective) model, it may well have use in choosing a Standard Earth Model, although the mathematical obstacles mentioned earlier would have to be overcome.

ACKNOWLEDGMENTS

I wish to thank David E. Smith for many helpful discussions and other valuable assistance. Discussions with Mike Graber were also very useful. Carl Wagner supplied the crustal models and the rock-equivalent topography. I thank Barbara Putney and Tom Odt for programming help. The support of the Director's Discretionary Fund of the Goddard Space Flight Center is gratefully acknowledged. The Technical Memorandum of Rubincam (1979) was erroneously numbered 80549. It should be 80586.

REFERENCES

- Anderson, D. L., The deep structure of continents, *J. Geophys. Res.*, **84**, 7555-7560, 1979.
- Arkani-Hamed, J., Lateral variations of density in the mantle, *Geophys. J. R. Astron. Soc.*, **20**, 431-455, 1970.
- Backus, G. E., and J. F. Gilbert, Numerical applications of a formalism for geophysical inverse problems, *Geophys. J. R. Astron. Soc.*, **13**, 247-276, 1967.
- Backus, G. E., and J. F. Gilbert, The resolving power of gross earth data, *Geophys. J. R. Astron. Soc.*, **16**, 169-205, 1968.
- Baierlein, R., *Atoms and Information Theory*, W. H. Freeman, San Francisco, 1971.
- Burg, J. P., Maximum entropy spectral analysis, paper presented at the 37th meeting of the Society of Exploration Geophysicists, Oklahoma City, OK, 1967.
- Burg, J. P., A new analysis for time series data, paper presented at the NATO Advanced Study Institute on Signal Processing with Emphasis on Underwater Acoustics, Enschede, Netherlands, 1968.
- Burg, J. P., The relationship between maximum entropy spectra and maximum likelihood spectra, *Geophysics*, **37**, 375-376, 1972.
- Burkhard, N., and D. D. Jackson, Application of stabilized linear inverse theory to gravity data, *J. Geophys. Res.*, **81**, 1513-1518, 1976.
- Cara, M., Lateral variations of S velocity in the upper mantle from higher Rayleigh modes, *Geophys. J. R. Astron. Soc.*, **57**, 649-670, 1979.
- Dziewonski, A. M., A. L. Hales, and E. R. Lapwood, Parametrically simple earth models consistent with geophysical data, *Phys. Earth Planet. Interiors*, **10**, 12-48, 1975.

- Dziewonski, A. M., B. H. Hager, and R. J. O'Connell, Large scale heterogeneities in the lower mantle, *J. Geophys. Res.*, **82**, 239-255, 1977.
- Graber, M. A., Polar motion spectra based upon Doppler, IPMS, and BIH data, *Geophys. J. R. Astron. Soc.*, **46**, 75-85, 1976.
- Graber, M. A., An information theory approach to the density of the earth, NASA/GSFC Tech. Memo. 78034, November, 1977.
- Gull, S. F., and G. J. Daniell, Image reconstruction from incomplete and noisy data, *Nature*, **272**, 686-690, 1978.
- Haxby, W. F., and D. L. Turcotte, On isostatic geoid anomalies, *J. Geophys. Res.*, **83**, 5473-5478, 1978.
- Hide, R., and K. Horai, On the topography of the core-mantle interface, *Phys. Earth/Planet. Interiors*, **1**, 305-308, 1968.
- Jaynes, E. T., Information theory and statistical mechanics, *Phys. Rev.*, Ser. 2, **106**, 620-630, and **108**, 171-190, 1957.
- Jaynes, E. T., Information theory and statistical mechanics, in *Statistical Physics*, edited by K. W. Ford, pp. 181-218, W. A. Benjamin, New York, 1963.
- Jaynes, E. T., Foundations of probability theory and statistical mechanics, in *Delaware Seminar in the Foundations of Physics*, edited by M. Bunge, pp. 77-101. Springer-Verlag, New York, 1967.
- Jordan, T. H., The continental tectosphere, *Rev. Geophys. Space Phys.*, **13**, no. 3, 1-12, 1975.
- Jordan, T. H., and J. N. Franklin, Optimal solutions to a linear inverse problem in geophysics, *Proc. Nat. Acad. Sci. USA*, **68**, 291-293, 1971.

- Julian, B. R., and M. K. Sengupta, Seismic travel time evidence for lateral inhomogeneity in the deep mantle, *Nature*, 242, 443-447, 1973.
- Katz, A., *Principles of Statistical Mechanics*, W. H. Freeman, San Francisco, 1967.
- Kaula, W. M., Elastic models of the mantle corresponding to variations in the external gravity field, *J. Geophys. Res.*, 68, 4967-4978, 1963.
- Kaula, W. M., Geophysical implications of satellite determinations of the earth's gravitational field, *Space Sci. Rev.*, 7, 769-794, 1967.
- Kaula, W. M., Global gravity and tectonics, in *The Nature of the Solid Earth*, edited by E. C. Robertson, J. F. Hays, and L. Knopoff, pp. 385-405, McGraw-Hill, New York, 1972.
- Kaula, W. M., Geophysical inferences from statistical analyses of the gravity field, in Dept. Geod. Sci. Rep. 250, pp. 119-141, Ohio State Univ., Columbus, 1977.
- Khan, M. A., Depth of sources of gravity anomalies, *Geophys. J. R. Astron. Soc.*, 48, 197-209, 1977.
- Koyama, J., Maximum entropy inversion of density structure of planets, *Science Reports of the Tohoku University*, Ser. 5, Geophysics, 26, 35-44, 1979.
- Lambeck, K., Gravity anomalies over ocean ridges, *Geophys. J. R. Astron. Soc.*, 30, 37-53, 1972.
- Lambeck, K., Lateral density anomalies in the upper mantle, *J. Geophys. Res.*, 81, 6333-6340, 1976.
- Lerch, F. J., C. A. Wagner, S. M. Klosko, and B. H. Putney, Goddard Earth Models for oceanographic applications (GEM 10B and 10C), *Marine Geodesy*, 5, 2-43, 1981.
- Lewis, B. T. R., and L. M. Dorman, Experimental isostasy, 2, An isostatic model for the U.S.A. derived from gravity and topographic data, *J. Geophys. Res.*, 75, 3367-3386, 1970.

- Lowman, P. D., A global tectonic activity map, *Bulletin of the International Association of Engineering Geology*, 23, 37-49, 1981.
- Lowrey, B. E., Lateral density anomalies and the earth's gravitational field, NASA/GSFC Tech. Memo, 79554, May 1978.
- Marsh, J. G., B. D. Marsh, R. G. Williamson, and W. T. Wells, The gravity field in the central Pacific from satellite-to-satellite tracking, *J. Geophys. Res.*, 86, 3979-3997, 1981.
- McQueen, H. W. S., and F. D. Stacey, Interpretation of low degree components of gravitational potential in terms of undulations of mantle phase boundaries, *Tectonophysics*, 34, T1-T8, 1976.
- Morse, P. M., *Thermal Physics*, second edition, W. A. Benjamin, New York, 1969.
- Nakiboglu, S. M., Hydrostatic figure and related properties of the earth, *Geophys. J. R. Astron. Soc.*, 57, 639-648, 1979.
- Parker, R. L., Understanding inverse theory, *Ann. Rev. Earth Planet. Sci.*, 5, 35-64, 1977.
- Phillips, R. J., and K. Lambeck, Gravity fields of the terrestrial planets: long-wavelength anomalies and tectonics, *Rev. Geophys. Space Phys.*, 18, 27-76, 1980.
- Reif, F., *Fundamentals of Statistical and Thermal Physics*, McGraw-Hill, New York, 1965.
- Rietsch, E., The maximum entropy approach to inverse problems, *J. Geophys.*, 42, 489-506, 1977.
- Romanowicz, B. A., Seismic structure of the upper mantle beneath the United States by three-dimensional inversion of body wave arrival times, *Geophys. J. R. Astron. Soc.*, 57, 479-506, 1979.

Rubincam, D. P., Information theory and the earth's density distribution, NASA/GSFC Tech. Memo. 78088, February 1978.

Rubincam, D. P., Information theory and the earth's density distribution—revised edition, NASA/GSFC Tech. Memo. 80586, August 1979.

Sabatier, P. C., On geophysical inverse problems and constraints, *J. Geophys.*, 43, 115-137, 1977.

Sanchez, B. V., Lateral density variations in elastic earth models from an extended minimum energy approach, NASA/GSFC Tech. Memo. 80742, June, 1980.

Shannon, C. E., A mathematical theory of communication, *Bell System Tech. J.*, 27, 379-423 and 623-656, 1948. (Reprinted in *The Mathematical Theory of Communication* by C. E. Shannon and W. W. Weaver, Univ. of Illinois Press, Urbana, IL, 1949.)

Smylie, D. E., G. K. C. Clarke, and T. J. Ulrych, Analysis of irregularities in the earth's rotation, in *Methods in Computational Physics*, 13, edited by B. A. Bolt, pp. 391-430, Academic Press, New York, 1973.

Tribus, M., *Thermostatistics and Thermodynamics*, Van Nostrand, New York, 1961.

Tribus, M., and R. Rossi, On the Kullback information measure as a basis for information theory: comments on a proposal by Hobson and Chang, *J. Stat. Phys.*, 9, 331-338, 1973.

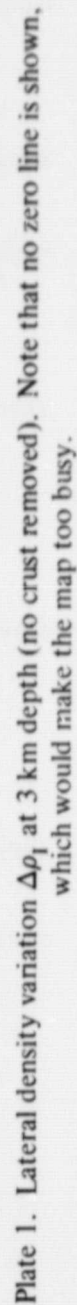


Plate 1. Lateral density variation $\Delta\rho_i$ at 3 km depth (no crust removed). Note that no zero line is shown, which would make the map too busy.

ORIGINAL PAGE
BLACK AND WHITE PHOTOGRAPH

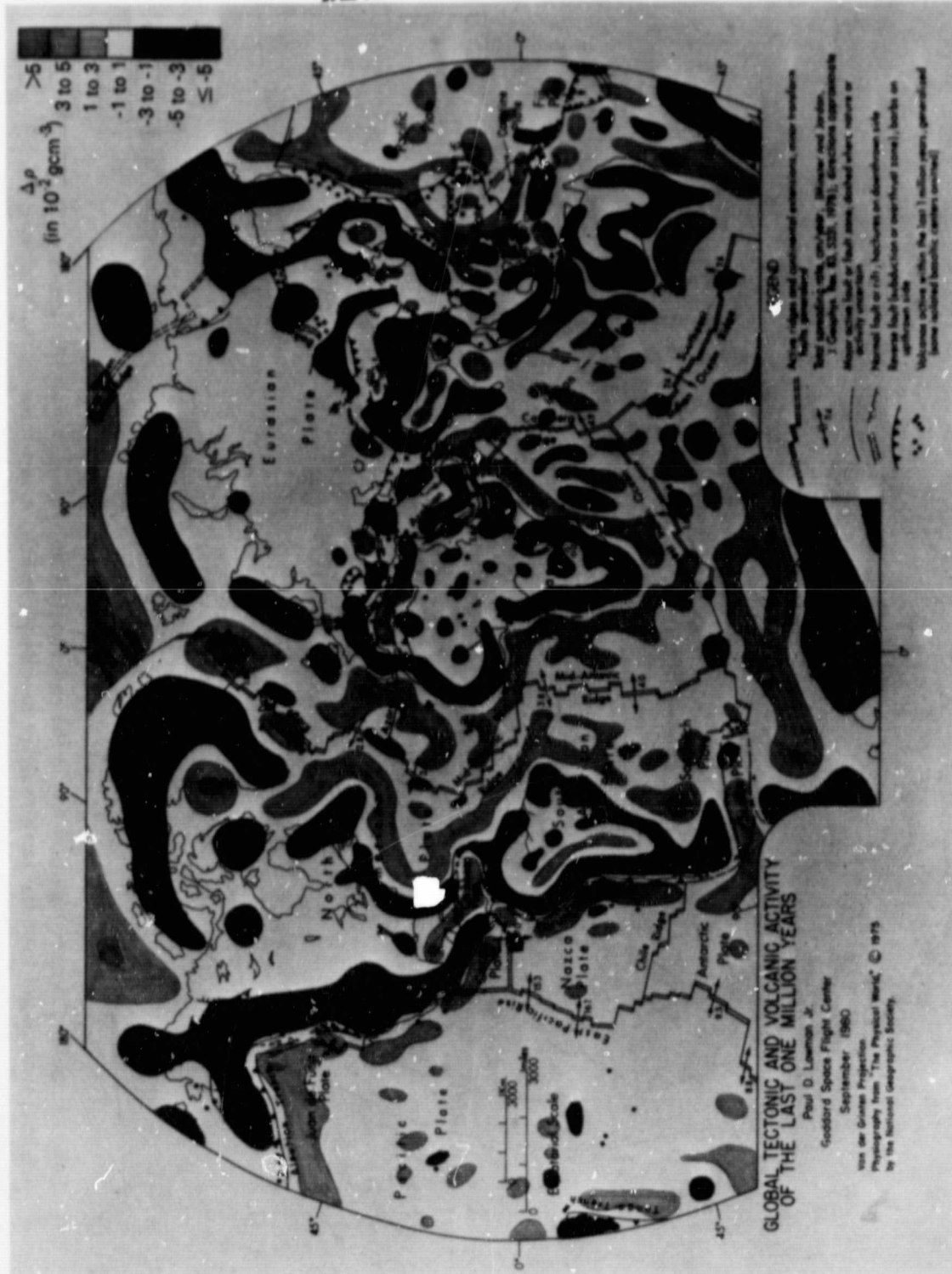


Plate 2. Lateral density variation $\Delta\rho_1$ at 30 km depth for 30 km of uncompensated crust removed.

Note that no zero line is shown, which would make the map too busy.

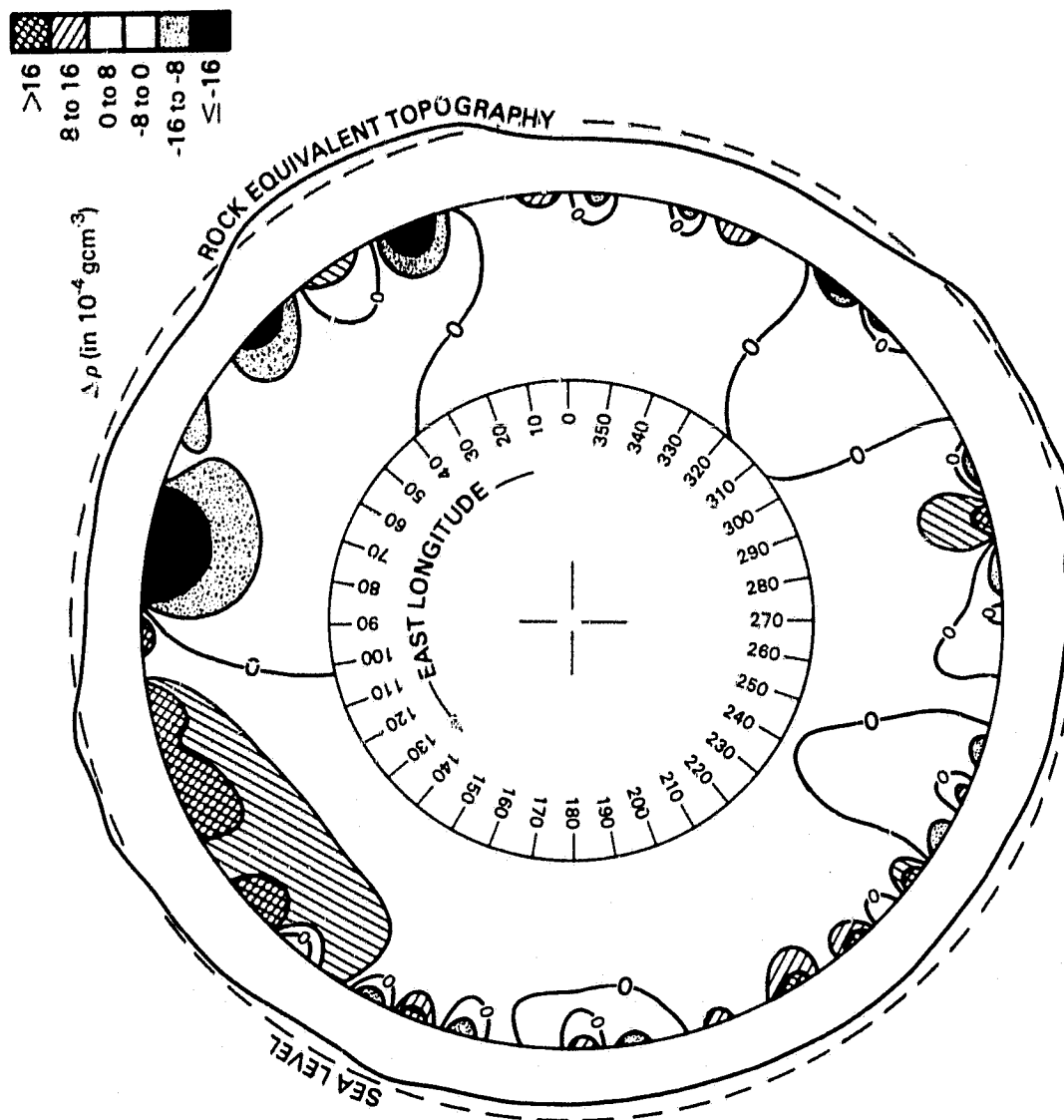


Figure 1. Lateral density variation $\Delta\rho_l$ in the equatorial plane of the earth for the case of no crust removed. Sea level is displaced from the earth's surface for clarity, and the rock-equivalent topography is greatly exaggerated. Anomalies in the core are not shown.

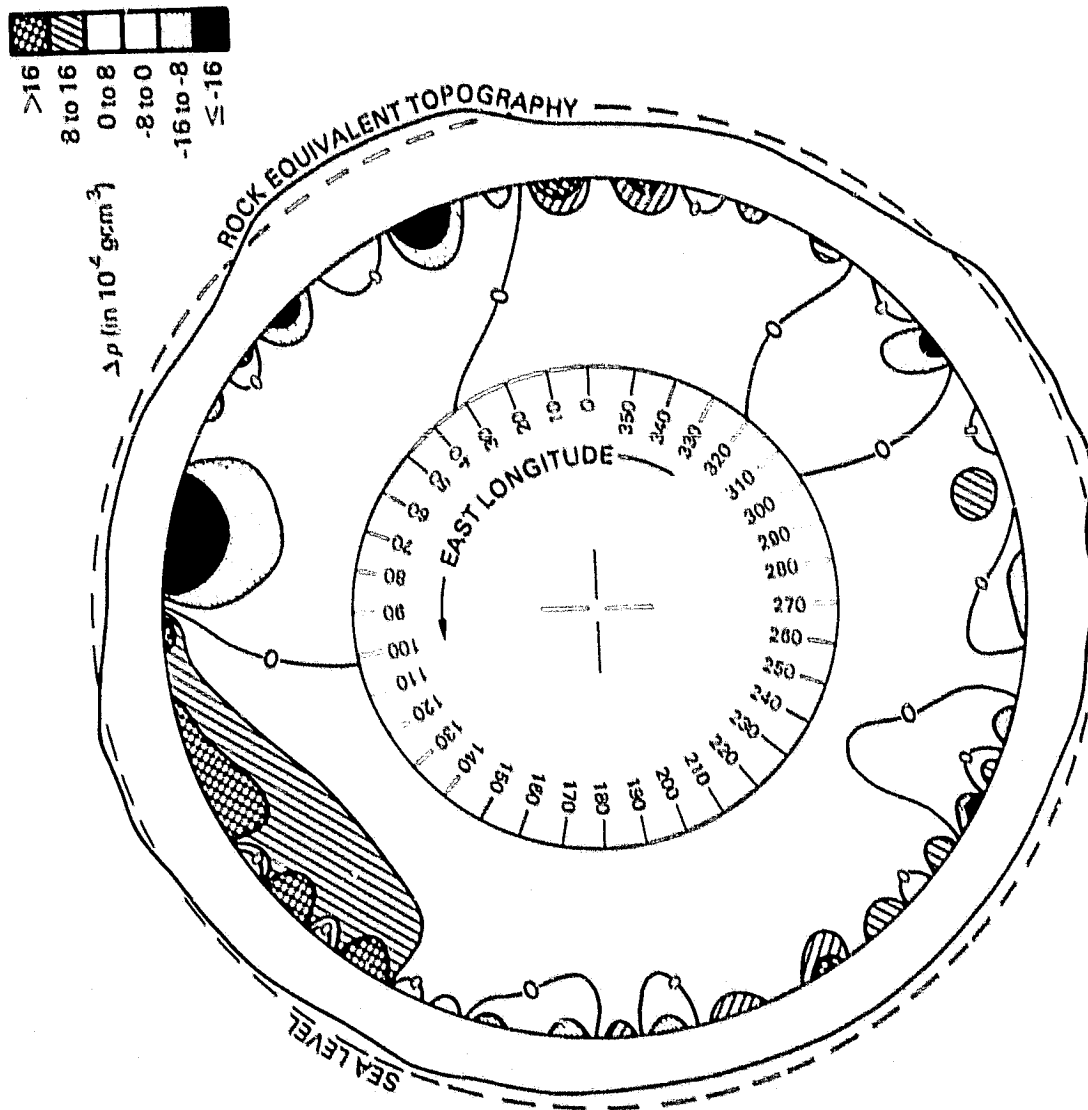


Figure 2. Lateral density variation $\Delta\rho_1$ in the equatorial plane of the earth for the case of 30 km of compensated crust removed. Sea level is displaced from the earth's surface for clarity, and the rock-equivalent topography is greatly exaggerated. Anomalies in the core are not shown.

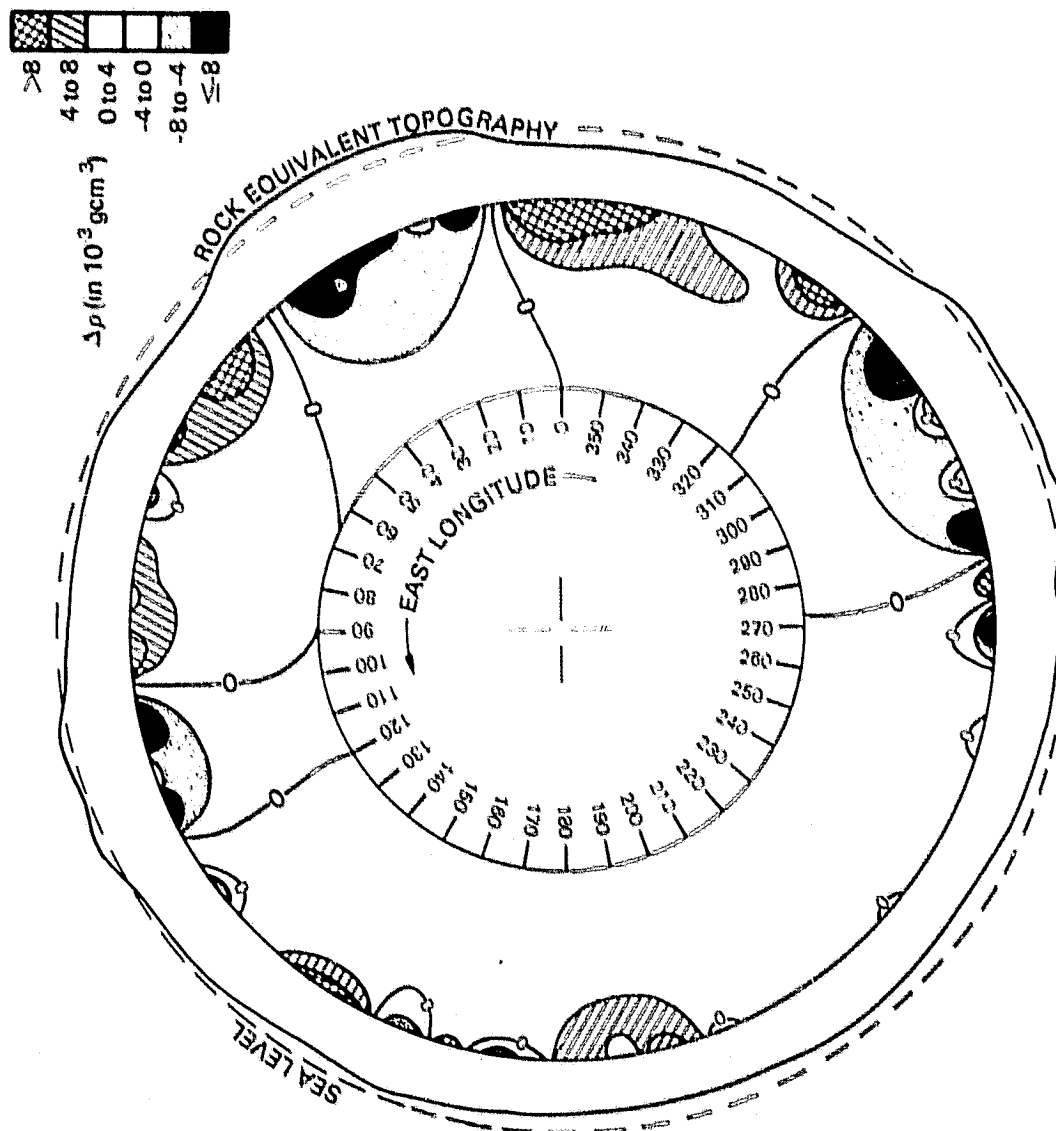


Figure 3. Lateral density variation $\Delta\rho_I$ in the equatorial plane of the earth for the case of 30 km of uncompensated crust removed. Sea level is displaced from the earth's surface for clarity, and the rock-equivalent topography is greatly exaggerated. Anomalies in the core are not shown.

FIGURE CAPTIONS

Plate 1. Lateral density variation $\Delta\rho_1$ at 3 km depth (no crust removed). Note that no zero line is shown, which would make the map too busy.

Plate 2. Lateral density variation $\Delta\rho_1$ at 30 km depth for 30 km of uncompensated crust removed. Note that no zero line is shown, which would make the map too busy.

Figure 1. Lateral density variation $\Delta\rho_1$ in the equatorial plane of the earth for the case of no crust removed. Sea level is displaced from the earth's surface for clarity, and the rock-equivalent topography is greatly exaggerated. Anomalies in the core are not shown.

Figure 2. Lateral density variation $\Delta\rho_1$ in the equatorial plane of the earth for the case of 30 km of compensated crust removed. Sea level is displaced from the earth's surface for clarity, and the rock-equivalent topography is greatly exaggerated. Anomalies in the core are not shown.

Figure 3. Lateral density variation $\Delta\rho_1$ in the equatorial plane of the earth for the case of 30 km of uncompensated crust removed. Sea level is displaced from the earth's surface for clarity, and the rock-equivalent topography is greatly exaggerated. Anomalies in the core are not shown.

Table 1

The Coefficients δ_ℓ for No Crust Removed ($R_U = 1$) and
30 km of Crust Removed ($R_U = 6341/6371$).

Degree ℓ	δ_ℓ	
	$R_U = 1$	$R_U = 6341/6371$
1	1.096	1.112
2	2.794	2.857
3	5.285	5.445
4	8.580	8.911
5	12.701	13.295
6	17.659	18.635
7	23.467	24.965
8	30.130	32.316
9	37.653	40.715
10	46.036	50.191
11	55.283	60.771
12	65.392	72.479
13	76.367	85.344
14	88.207	99.393
15	100.913	114.653
16	114.486	131.152
17	128.929	148.920
18	144.241	167.987
19	160.426	188.382
20	177.485	210.138
21	195.421	233.286
22	214.235	257.858
23	233.931	283.890
24	254.510	311.414
25	275.976	340.466
26	298.332	371.082
27	321.579	403.298
28	345.722	437.152
29	370.763	472.681
30	396.706	509.925
31	423.552	548.922
32	451.306	589.713
33	479.971	632.339
34	509.548	676.842
35	540.043	723.263
36	571.458	771.647

APPENDIX

Finding the variance $\sigma_n^2 = \langle n_j^2 \rangle - \langle n_j \rangle^2$ from (8) closely follows the standard statistical mechanics treatment (e.g., Reif, 1965, pp. 336-337). It is given by

$$\sigma_n^2 = \frac{\partial^2 \ln Z}{\partial (\alpha_1 f_1(\vec{r}_j))^2}$$

which gives

$$\frac{\sigma_n}{\langle n_j \rangle} = \sqrt{1 + \frac{1}{\langle n_j \rangle}} = \frac{\sigma_\rho}{\rho(\vec{r})}, \quad \sigma_\rho = \frac{m}{dv} \sigma_n$$

for particles following Bose-Einstein statistics (Reif, 1965, p. 346; Morse, 1969, p. 333). Because it is assumed that $\langle n_j \rangle \ll 1$, all that can be said about σ_ρ is that $\sigma_\rho > \rho(\vec{r})$, since no commitment to the value of $\langle n_j \rangle$ has been made. Hence the data do not greatly constrain the density distribution.

PRECEDING PAGE BLANK NOT FILMED

APPENDIX B

The computer program used to generate the plates and figures is listed here. Plates 1 and 2 use subroutine VANDER. Figures 1, 2, and 3 use subroutine SLICE.

C	*INFORMATION THEORY DENSITY DISTRIBUTION*	MAI	1
C	THIS PROGRAM COMPUTES THE INFORMATION THEORY DENSITY DISTRIBUTION	MAI	2
C	BASED ON THE GRAVITY FIELD. IT ASSUMES MAXWELL-BOLTZMANN STATISTICS	MAI	3
C	AND THAT THE SPHERICALLY SYMMETRIC PART OF THE DENSITY DISTRIBUTION	MAI	4
C	IS KNOWN.	MAI	5
C	THE PROGRAM USES SPHERICAL HARMONICS. THE LATERAL DENSITY	MAI	6
C	VARIATION IS ASSUMED TO BE A SMALL PERTURBATION ON TOP OF THE	MAI	7
C	SPHERICALLY SYMMETRIC DENSITY DISTRIBUTION.	MAI	8
C	THE PROGRAM COMPUTES THE DENSITY VARIATION, RELATIVE DENSITY, OR	MAI	9
C	ACTUAL DENSITY INSIDE THE EARTH, WHICH MAY BE DISPLAYED IN VARIOUS	MAI	10
C	WAYS ACCORDING TO A CHOSEN SUBROUTINE. THE DISPLAY IS IN ONE OF TWO	MAI	11
C	MODES: PRINT-OUT PICTURES OR DICED PHOTOGRAPHS.	MAI	12
C	THE DENSITY IS DEFINED AS THE SPHERICALLY SYMMETRIC PART	MAI	13
C	(RHO SUB-ZERO) PLUS THE DENSITY VARIATION (DELTA RHO). THE RELATIVE	MAI	14
C	DENSITY IS DEFINED AS DELTA RHO DIVIDED BY RHO SUB-ZERO.	MAI	15
C	CRUSTAL MODELS (SUCH AS AN ISOSTATICALLY COMPENSATED CRUST OR	MAI	16
C	AN ISOSTATICALLY UNCOMPENSATED CRUST) MAY BE SUBTRACTED OFF IF	MAI	17
C	DESIRED AND THE INFORMATION THEORY ALGORITHM APPLIED TO THE REMAINING	MAI	18
C	GRAVITY SIGNAL.	MAI	19
C	ALSO, THE DEGREES USED BY THE SPHERICAL HARMONIC FIELDS CAN BE	MAI	20
C	RESTRICTED TO A CERTAIN RANGE (BETWEEN LMIN AND LMAX INCLUSIVE) IF	MAI	21
C	SO DESIRED.	MAI	22
C	NCTATION	MAI	23
C	GENERAL DATA	MAI	24
C	PI = 3.1415926535897900	MAI	25
C	PIDIV2 = PI/2.000	MAI	26
C	PI2 = 2.000*PI	MAI	27
C	LLOW = MINIMUM DEGREE OF GRAVITY/TOPOGRAPHY/CRUSTAL FIELD	MAI	28
C	RECORDS READ	MAI	29
C	LUP = MAXIMUM DEGREE OF GRAVITY/TOPOGRAPHY/CRUSTAL FIELD	MAI	30
C	RECORDS READ	MAI	31
C	LPTN = MINIMUM DEGREE OF GRAVITY/TOPOGRAPHY/CRUSTAL FIELD	MAI	32
C	TO BE USED IN PROGRAM	MAI	33
C	LMAX = MAXIMUM DEGREE OF GRAVITY/TOPOGRAPHY/CRUSTAL FIELD	MAI	34
C	TO BE USED IN PROGRAM	MAI	35
C	SUBNME = NAME OF SUPROUTINE CALLED	MAI	36
C	COMENT = GENERAL COMMENTS ABOUT PARTICULAR RUN (SUCH AS THE NAME	MAI	37
C	OF THE REGION BEING EXAMINED, ETC)	MAI	38
C	NPRINT = 1 IF GRAVITY/TOPOGRAPHY/CRUSTAL FIELD COEFFICIENTS ARE	MAI	39
C	TO BE LISTED, =0 IF NOT	MAI	40
C	EARTH DATA	MAI	41
C	RHOAVG = AVERAGE DENSITY OF THE EARTH IN GRAMS/CM**3	MAI	42
C	RADAVG = AVERAGE RADIUS OF EARTH IN KILOMETERS	MAI	43
C	RCORKM = RADIUS OF OUTER CORE IN KILOMETERS	MAI	44
C	RCORE = RCORKM/RADAVG	MAI	45
C	RLOWKM = LOWER RADIAL LIMIT ALLOWED FOR DENSITY ANOMALIES, IN	MAI	46
C	KILOMETERS	MAI	47
C	RLOWER = RLOWKM/RADAVG	MAI	48
C	RUPKM = UPPER RADIAL LIMIT ALLOWED FOR DENSITY ANOMALIES, IN	MAI	49
C	KILOMETERS	MAI	50
C	RUPPER = RUPKM/RADAVG	MAI	51
C	GRAVITY FIELD	MAI	52
C	GRAV = DESCRIPTION OF GRAVITY FIELD	MAI	53
C	CRUST	MAI	54
C	CCRUST = DESCRIPTION OF CRUSTAL MODEL	MAI	55
C	NCRUST = 1 IF CRUSTAL MODEL FIELD IS SUBTRACTED FROM GRAVITY	MAI	56
C	FIELD, =0 IF NOT	MAI	57
C	TOPOGRAPHY	MAI	58
C	TOPO = DESCRIPTION OF TOPOGRAPHY	MAI	59
C	TOPC = ARRAY IN WHICH TOPOGRAPHY COEFFICIENTS ARE STORED	MAI	60
C	LATERAL DENSITY DISTRIBUTION	MAI	61
C	COMPT = REMARKS ABOUT THE COE(L) (SUCH AS THE DEPTHS FOR WHICH	MAI	62

ORIGINAL PAGE IS OF POOR QUALITY

C	THEY WERE (OPLTED)	PAI	63
C	CCE = INFORMATION-THEORETIC CCEFFICIENTS BASED ON THE	PAI	64
C	SPHERICALLY SYMMETRIC DENSITY DISTRIBUTION	PAI	65
C	CLM = INFORMATION-THEORETIC RELATIVE DENSITY/DENSITY/DENSITY	PAI	66
C	VARIATION SPHERICAL HARMONIC COEFFICIENTS	PAI	67
C	NDEA = 0 IF RELATIVE DENSITY DISTRIBUTION IS PLOTTED, =1 IF	PAI	68
C	ACTUAL DENSITY IS PLOTTED, =2 IF DENSITY VARIATION IS	PAI	69
C	PLOTTED	PAI	70
C	REFDEN = REFERENCE DENSITY, USED ONLY IF NDEN=1	PAI	71
C	PICTURE DATA	PAI	72
C	NPHCTC = 0 IF PRINT-OUT PICTURE IS DESIRED, =1 IF DICOMED	PAI	73
C	PHOTOGRAPH IS DESIRED	PAI	74
C	MAXSYM = NUMBER OF ALPHANUMERIC SYMBOLS USED FOR PRINT-OUT	PAI	75
C	PICTURE OR DICOMED PHOTO	PAI	76
C	ALPHA = ARRAY IN WHICH ALPHANUMERIC SYMBOLS USED FOR PRINT-OUT	PAI	77
C	PICTURES ARE STORED, IN ORDER FROM LOW TO HIGH	PAI	78
C	RELATIVE DENSITY/DENSITY/DENSITY VARIATION	PAI	79
C	BETA = ARRAY IN WHICH DICOMED COLOR CODING NUMBERS ARE	PAI	80
C	STORED, USED FOR DICOMED PHOTO, IN ORDER FROM LOW	PAI	81
C	TO HIGH RELATIVE DENSITY/DENSITY/DENSITY VARIATION	PAI	82
C	SCALE = RELATIVE DENSITY/DENSITY/DENSITY VARIATION INTERVAL	PAI	83
C	BETWEEN ALPHANUMERIC SYMBOLS (OR COLORS)	PAI	84
C	(UNITS: NONE IF NDEN=0, GRAMS/CM**3 IF NDEN=100 2)	PAI	85
C	SUBROUTINES CALLED:	PAI	86
C	1. CUTS (IF SUBNPE .EQ. CUT)	PAI	87
C	2. PIECE (IF SUBNPE .EQ. PIE)	PAI	88
C	3. POLES (IF SUBNPE .EQ. POL)	PAI	89
C	4. SECTNS (IF SUBNPE .EQ. SEC)	PAI	90
C	5. SLICE (IF SUBNPE .EQ. SLI)	PAI	91
C	6. VANDER (IF SUBNPE .EQ. VAN)	PAI	92
C	NOTES	PAI	93
C	1. ALL SPHERICAL HARMONIC FIELDS (GRAVITY, TOPOGRAPHIC, CRUSTAL)	PAI	94
C	USE KAULA'S 4*PI NORMALIZATION.	PAI	95
C	2. THE TOPOGRAPHIC FIELD IS NORMALIZED TO THE RADIUS OF THE	PAI	96
C	EARTH (IN KILOMETERS).	PAI	97
C	3. THE FOLLOWING CONDITIONS MUST BE SATISFIED:	PAI	98
C	LMIN .GE. LLOW	PAI	99
C	LMAX .LE. LUP	PAI	100
C	4. THE DENSITY VARIATION OR RELATIVE DENSITY IS MORE CONVENIENT	PAI	101
C	TO DISPLAY THAN THE ACTUAL DENSITY.	PAI	102
C	5. IF WE HAVE ALPHA(JNL*) WHERE JNUM .GT. MAXSYM, THEN THE	PAI	103
C	PROGRAM SETS JNLM=MAXSYM. ALSO, IF JNUM .LT. 1, THEN WE SET	PAI	104
C	JNUM=1. LIKEWISE FOR BETA(JNLM).	PAI	105
C	IN OTHER WORDS, IF THE RELATIVE DENSITY/DENSITY/DENSITY	PAI	106
C	VARIATION GOES OFF SCALE AT EITHER END, THEN THE LIMIT AT	PAI	107
C	THAT END IS USED.	PAI	108
C	6. PROGRAM NORMALIZES ALL RADIAL DISTANCES BY DIVIDING RADIAL	PAI	109
C	DISTANCE (IN KILOMETERS) BY RADAVG.	PAI	110
C	SAMPLE INPUT DATA (COLUMN 1 OF INPUT STARTS IN COLUMN 3 HERE)	PAI	111
C	LLOW LUP	(FORMAT: 415)	PAI 112
C	36 36		PAI 113
C	LMIN LMAX	(FORMAT: 415)	PAI 114
C	36 36		PAI 115
C	ACRUST APRINT	(FORMAT: 415)	PAI 116
C	1 1		PAI 117
C	RADAVG RCORRM RHCAVG	(FORMAT: 8F10.5)	PAI 118
C	6371.0 3485.7 5.517		PAI 119
C	(COMPN1(J), J=1,14)	(FORMAT: 13A6,A2)	PAI 120
C	DENSITY CCEFFICIENTS COE(I) (RANGE: 670 TO 30 KM DEPTH)		PAI 121
C	RLOWRM RUPKM	(FORMAT: 8F10.5)	PAI 122
C	5701.0 6341.0		PAI 123
C	K COE(K)	(FORMAT: 15,F20.6)	PAI 124
C	1 3.4505062		PAI 125
C	2 6.4100380		PAI 126
C	...		PAI 127
C	35 723.66557		PAI 128
C	36 771.99419		PAI 129
C	(GPAV(J), J=1,14)	(FORMAT: 13A6,A2)	PAI 130

ORIGINAL PAGE IS
OF POOR QUALITY

```

C GENI08, USING MAX(ROGLU(1974) HYDROSTATIC FOR L=2,4; M=0          MAI 131
C
C      L M C S (FORMAT: 6X,212,2015.0) MAI 132
C      1 0 0.0 0.0 MAI 133
C      1 1 0.0 0.0 MAI 134
C      *** MAI 135
C      3635 0.359901570-(8-0.731970240-08 MAI 136
C      3636 0.249368180-(8-0.886649470-09 MAI 137
C      (TTOPO(J), J=1,14) (FORMAT: 13A6,A2) MAI 138
C ROCK-EQUIVALENT TOPOGRAPHY - NORMALIZED TO RADIUS OF THE EARTH MAI 139
C
C      L M C S (FORMAT: 6X,212,2015.0) MAI 140
C RECCE1 1 0 0.731720180-C4 0.0 MAI 141
C RECCE1 1 1 0.63249042C-C4 0.42260593C-04 MAI 142
C      *** MAI 143
C RECCE13635 0.145268950-(5-0.776859170-06 MAI 144
C RECCE13636 0.72330886C-(6-0.2402089RC-06 MAI 145
C      (CCRUST1(J), J=1,14) (FORMAT: 13A6,A2) MAI 146
C GRAVITY COEFFICIENTS-UNCOMPENSATED CRUST, FROM KAULA&LEE, SCRIPPS, NAVY MAI 147
C
C      L M C S (FORMAT: 214,1P2C15.6) MAI 148
C      1 0 3.4352110-C4 0.0 MAI 149
C      1 1 2.987885C-04 2.0724950-C4 MAI 150
C      *** MAI 151
C      36 35 3.5216880-C7 -2.2664080-C7 MAI 152
C      36 36 5.4404990-C8 -1.1692660-C7 MAI 153
C
C NPHOTO MAXSYM SCALE (FORMAT: 215,F10.5) MAI 154
C      0 20 0.001 MAI 155
C
C (ALPHA1(J), J=1,21) (FORMAT: 21A1) MAI 156
C JHGFEDCBA123456789+ MAI 157
C
C (BETA1(J), J=1,11) (FORMAT: 11I3) MAI 158
C      7 8 9 10 31 20 19 18 17 22 1 MAI 159
C
C NDEN RECDEN (FORMAT: 15,F20.9) MAI 160
C      0 0.0 MAI 161
C      *** MAI 162
C (FOR THE REST OF THE SAMPLE INPUT, WHICH RELATES TO THE MAI 163
C PARTICULAR SUBROUTINE CALLED, SEE THE SUBROUTINE.) MAI 164
C
C
C IMPLICIT REAL*8(A-M,O-Z) MAI 165
C INTEGER*2 BETA(11) MAI 166
C DIMENSION ALPHA(23),LCWF(1205,2) MAI 167
C DIMENSION COMENT (14) MAI 168
C DIMENSION CLM(36,37,2),COM(136) MAI 169
C DIMENSION TOPO(136,37,2) MAI 170
C DIMENSION COMENT(14),GRAV(14),CCRUST(14),TTOPO(14) MAI 171
C COMMON/BLKB/CLM,CCE MAI 172
C COMMON/BLKG/F,P1,P12,PICIV2,SCALE,NPHOTO,MAXSYM MAI 173
C COMMON/BLKD/ALPHA,LCWF MAI 174
C COMMON/BLKG/LMIN,LMAX,LLOW,LUP MAI 175
C COMMON/BLKH/RADAVG,RCORE,RLOWER,RUPPER MAI 176
C COMMON/BLKI/COMENT MAI 177
C COMMON/BLKJ/NDEN,RECDEN MAI 178
C COMMON/BLKK/TOPO MAI 179
C COMMON/BLKT/BETA MAI 180
C DATA POL,PIE/6HP0LES ,6+PIECE / MAI 181
C DATA SLI,SEC,VAN/6HSLICE ,6HSECTNS,6HVANDER/ MAI 182
C DATA CUT/6HCUTS / MAI 183
C DATA BLANK,DOLLAR/1+ ,1+8/ MAI 184
C
C SUPPRESS UNDERFLOW ERROR MESSAGES CN SUBROUTINE LGENDR MAI 185
C CALL ERRSET(208,256,-1,1) MAI 186
C
C INITIALIZE BASIC CONSTANTS MAI 187
C P1=3.14159265358979C0 MAI 188
C F=PI/180.000 MAI 189
C P12=2.0COP1 MAI 190
C PICIV2=PI/2.000 MAI 191
C ALPHA(22)=DOLLAR MAI 192
C ALPHA(23)=BLANK MAI 193
C
C READ IN BASIC DATA MAI 194
C READ (5,17) LLOW,LUP MAI 195
C 17 FCRMAT (415) MAI 196
C READ (5,17) LMIN,LMAX MAI 197
C READ (5,17) NCRUST,NPRINT MAI 198
C
C READ (5,104) RADAVG,RCORPM,RHOAVG MAI 199
C RCORE=RCORPM/RADAVG MAI 200
C
C SET DATA ARRAYS INITIALLY EQUAL TO ZERO MAI 201

```

MPAX=LMAX + 1	PAI	202
DC 23 L=1,LMAX	PAI	203
CCEIL=C.OCC	PAI	204
DC 23 M=1,MPAX	PAI	205
TCPCIL,M,1)=0.000	PAI	206
TCPCIL,M,2)=0.000	PAI	207
CLM(L,M,1)=0.000	PAI	208
CLM(L,M,2)=0.000	PAI	209
C		
READ IN CCE(L) DATA	PAI	210
READ (5,25) (GCMPT(J), J=1,14)	PAI	211
FCMPAT (13A6,A2)	PAI	212
C		
READ (5,104) RLCKM,RLPKM	PAI	213
FCMPAT (BF10,5)	PAI	214
RLCWR=RLCKM/RADAVC	PAI	215
RUPPER=RUPKM/RADAVC	PAI	216
C		
ICCLAT=0	PAI	217
DC 24 L=LMIN,LMAX	PAI	218
READ(5,21) K,CCEIK)	PAI	219
FCMPAT (15,F20,9)	PAI	220
ICCLAT=ICCLAT + 1	PAI	221
CONTINUE	PAI	222
C		
READ IN GRAVITY FIELD C'S AND S'S	PAI	223
C		
READ (5,25) (GRAV(J), J=1,14)	PAI	224
WRITE (6,14)	PAI	225
WRITE (6,32)	PAI	226
32 FCMPAT (20X,'GRAVITY FIELD COEFFICIENTS',/)	PAI	227
WRITE (6,33) (GRAV(J), J=1,14)	PAI	228
33 FCMPAT (20X,13A6,A2,///)	PAI	229
WRITE (6,34)	PAI	230
34 FCMPAT (10X,' L',2X,' M',9X,'C',10X,'S',/)	PAI	231
JCOUNT=0	PAI	232
2 READ (5,1,END=3) L,P,C,S	PAI	233
1 FCMPAT (6X,212,2015,8)	PAI	234
IF (INPRINT .EQ. 0) GO TO 331	PAI	235
C WRITE GRAVITY FIELD C'S AND S'S	PAI	236
WRITE (6,35) L,P,C,S	PAI	237
35 FCMPAT (10X,12,2X,12,2X,015,8,2X,015,8)	PAI	238
331 JCOUNT=JCOUNT + 1	PAI	239
IF (L .GT. LMAX) GO TO 13	PAI	240
IF (L .LT. LMIN) GO TO 13	PAI	241
C COMPUTE DENSITY DISTRIBUTION COEFFICIENTS	PAI	242
CCEFF=RADAVG*(CCEIL)	PAI	243
M=M + 1	PAI	244
CLM(L,M,1)=C*CCEFF	PAI	245
CLM(L,M,2)=S*CCEFF	PAI	246
IF (L .EQ. LUP .AND. M .EQ. LUP) GO TO 3	PAI	247
13 CONTINUE	PAI	248
GO TO 2	PAI	249
3 CONTINUE	PAI	250
WRITE (6,120) JCOUNT	PAI	251
120 FCMPAT (7,10X,'NUMBER OF GRAVITY FIELD RECORDS READ:',1X,110)	PAI	252
C		
READ IN TOPOGRAPHIC C'S AND S'S	PAI	253
C		
READ (5,25) (TTOPC(J), J=1,14)	PAI	254
WRITE (6,14)	PAI	255
WRITE (6,321)	PAI	256
321 FCMPAT (20X,'TOPOGRAPHY COEFFICIENTS',/)	PAI	257
WRITE (6,33) (TTOPC(J), J=1,14)	PAI	258
WRITE (6,34)	PAI	259
LCOUNT=0	PAI	260
322 READ (5,1,END=324) L,P,C,S	PAI	261
IF (INPRINT .EQ. 0) GO TO 332	PAI	262
C WRITE TOPOGRAPHIC C'S AND S'S	PAI	263
WRITE (6,35) L,P,C,S	PAI	264
332 LCOUNT=LCOUNT + 1	PAI	265
IF (L .GT. LMAX) GO TO 323	PAI	266
IF (L .LT. LMIN) GO TO 323	PAI	267
M=M + 1	PAI	268
TCPCIL,M,1)=C	PAI	269
TCPCIL,M,2)=S	PAI	270
IF (L .EQ. LUP .AND. M .EQ. LUP) GO TO 324	PAI	271
323 CONTINUE	PAI	272
GO TO 322	PAI	273
324 CONTINUE	PAI	274
WRITE (6,125) LCOUNT	PAI	275
125 FCMPAT (7,10X,'NUMBER OF TOPOGRAPHY RECORDS READ:',3X,110)	PAI	276
C		
IF (INCRUST .EQ. 0) JCOUNT=0	PAI	277
IF (INCRUST .EQ. 0) GO TO 43	PAI	278
C		
READ IN CRUSTAL C'S AND S'S	PAI	279
C		

ORIGINAL PAGE IS
OF POOR QUALITY

```

      READ (5,25) (CCRUST(J), J=1,14)
      WRITE (6,14)
      WRITE (6,26) (CCRLST(J), J=1,14)
      KCOLAT=0
      WRITE (6,34)
41  REAC (5,42,END=43) L,P,C,S
42  FORMAT (2I4,1P2D15.4)
      IF (INPRINT .EQ. 0) GO TO 333
C   WRITE OUT CRUSTAL C'S AND S'S
      WRITE (6,35) L,P,C,S
333  KCOLAT=KCOUNT + 1
      IF (L .GT. LMAX) GO TO 52
      IF (L .LT. LMIN) GO TO 52
      CCEFF=H*DAVG*(CCE(L))
      M1=1
C   SUBTRACT CRUSTAL FIELD FROM DENSITY COEFFICIENTS
      CLP(L,M1,1)=CLM(L,M1,1) - C*CCEFF
      CLP(L,M1,2)=CLM(L,M1,2) - S*CCEFF
      IF (L .EQ. LUP .AND. P .EQ. LUP) GO TO 43
52  CONTINUE
      GO TO 41
43  CONTINUE
      WRITE (6,121) KCOUNT
121  FORMAT (I,10X,'NUMBER OF CRUSTAL FIELD RECORDS READ:',I,X,110)
C
C   READ IN DISPLAY DATA
      REAC (5,201) NPHOTO,MAXSYM,SCALE
201  FORMAT (2I5,7F10.5)
      REAC (5,50) (ALPHA(J), J=1,21)
50  FORMAT (21A1)
      REAC (5,51) (BETA(J), J=1,11)
51  FORMAT (11I3)
      REAC (5,21) NDEN,REYDEN
C
C   WRITE OUT INPUT DATA
C
      WRITE (6,14)
      WRITE (6,300)
300  FORMAT (20X,'INFORMATION THEORY DENSITY DISTRIBUTION',/,20X,
. 'BASED ON THE GRAVITY FIELD COEFFICIENTS',/,20X,
. 'AND KNOWN SPHERICALLY SYMMETRIC DENSITY DISTRIBUTION',/,,/)
      WRITE (6,340) LLOW
340  FORMAT (10X,'LLOW=',I4,20X,'(MINIMUM DEGREE OF SPHERICAL HARMONIC
. 'FIELDS)',/)
      WRITE (6,341) LUP
341  FORMAT (10X,'LUP =',I4,20X,'(MAXIMUM DEGREE OF SPHERICAL HARMONIC
. 'FIELDS)',/)
      WRITE (6,342) LMIN
342  FORMAT (10X,'LMIN=',I4,20X,'(MINIMUM DEGREE USED IN RUN)',/)
      WRITE (6,343) LMAX
343  FORMAT (10X,'LMAX=',I4,20X,'(MAXIMUM DEGREE USED IN RUN)',/)
      WRITE (6,303) NCRUST
303  FORMAT (10X,'NCRUST=',I2,20X,'(=1 IF CRUSTAL MODEL IS SUBTRACTED;
. '0 IF NOT)',/)
      WRITE (6,330) NPRINT
330  FORMAT (10X,'NPRINT=',I2,20X,'(=1 IF GRAVITY, TOPOGRAPHIC, AND CRUSTAL
. 'FIELD COEFFICIENTS ARE PRINTED; 0 IF NOT)',/)
      WRITE (6,304) RADAVG
304  FORMAT (10X,'RADAVG=',I,X,F10.3,I,X,'KM',10X,'(AVERAGE RADIUS OF EARTH)
. 'IN CM',/)
      WRITE (6,305) RCORCM
305  FORMAT (10X,'RCORCM=',I,X,F10.3,I,X,'KM',10X,'(RADIUS OF CORE)',/)
      WRITE (6,306) RHOAVG
306  FORMAT (10X,'RHOAVG=',I,X,F10.5,I,X,'GRAM/CM**3',10X,'(AVERAGE DENSITY
. 'OF EARTH)',/)
      WRITE (6,307) RLOWKM
307  FORMAT (10X,'RLOWKM=',I,X,F10.3,I,X,'KM',10X,'(LOWER BOUND ON ANOMALY
. 'IN CM)',/)
      WRITE (6,308) RUPKM
308  FORMAT (10X,'RUPKM=',I,X,F10.3,I,X,'KM',10X,'(UPPER BOUND ON ANOMALY
. 'IN CM)',/)
      WRITE (6,309) NPHOTO
309  FORMAT (10X,'NPHOTO=',I2,20X,'(=1 IF PHOTO IS TAKEN; 0 FOR PRINT-OUT
. 'PICTURE)',/)
      WRITE (6,311) SCALE
311  FORMAT (10X,'SCALE=',I,X,F10.5,22X,'(UNITS: NONE IF NDEN=0, GRAM/CM**3
. 'IF NDEN=1 OR 2)',/)
      WRITE (6,310) MAXSYM
310  FORMAT (10X,'MAXSYM=',I2,27X,'(NUMBER OF ALPHANUMERIC SYMBOLS USED)
. 'IN TITLE',/)
      WRITE (6,312) (ALPHA(J), J=1,21)
312  FORMAT (10X,'ALPHA(J):',I,X,21A1, 8X,'(FROM LOW TO HIGH DENSITY)',/,,)
      WRITE (6,313) (BETA(J), J=1,11)
313  FORMAT (10X,'BETA(J):',I,X,11I3,1X,10X,'(USED FOR PHOTO)',/)
      WRITE (6,314) NDEN
314  FORMAT (10X,'NDEN=',I3,31X,'(=0 FOR RELATIVE DENSITY, =1 FOR ACTUAL
. 'DENSITY, =2 FOR DENSITY VARIATION)',/)

```

	WRITE (6,317) REFCEA	PAI	365
317	FORMAT (10X,'REFDEN=',1X,F10.7,1X,'GHAN/CM**3',10X,'(REFERENCE DENMAI	MAI	366
	SITY, USED WHEN NCEA=1)',//)	PAI	367
	WRITE (6,326)	PAI	368
326	FORMAT (//,10X)	MAI	369
	WRITE (6,315) (GRAV(J), J=1,14)	MAI	370
315	FORMAT (10X,'GRAVITY FIELD:',1X,13A6,A2)	MAI	371
	WRITE (6,120) JCOUNT	MAI	372
	WRITE (6,325) (TTEPC(J), J=1,14)	MAI	373
325	FORMAT (//,10X,'TTEPCORAFHY',3X,'',1X,13A6,A2)	PAI	374
	WRITE (6,125) LCOUNT	MAI	375
	IF (INCRUST.EQ. 0) GO TO 318	PAI	376
	WRITE (6,316) (CCPUST(J), J=1,14)	PAI	377
316	FORMAT (//,10X,'CHUST',EX,'',1X,13A6,A2)	PAI	378
	WRITE (6,121) KCOUNT	MAI	379
	GO TO 319	PAI	380
318	WRITE (6,320)	PAI	381
320	FORMAT (//,10X,'CHUST',EX,'',1X,'NO CRUSTAL MODEL SUBTRACTED OUT'	MAI	382
	.)	MAI	383
319	CONTINUE	PAI	384
C			
C	WRITE CUT COE(L)	MAI	385
	WRITE (6,14)	MAI	386
14	FORMAT (1H1)	PAI	387
	WRITE (6,26) (COMPNT(J), J=1,14)	MAI	388
26	FORMAT (10X,13A6,A2,//)	PAI	389
C			
	WRITE (6,29)	MAI	390
29	FORMAT (24X,'L',2CX,'COE(L)',//)	MAI	391
	DO 30 L=LMIN,LMAX	MAI	392
30	WRITE (6,31) L,COE(L)	MAI	393
31	FORMAT (20X,15,10X,F2C.5)	MAI	394
	WRITE (6,122) LCOUNT	MAI	395
122	FORMAT (//,9X,'NUMBER OF COE(L) RECORDS READ:',1X,I10)	PAI	396
C			
C			
C	READ IN SUBROUTINE NAPE	PAI	397
	REAC (5,49) SUBNAME	MAI	398
49	FORMAT (A6)	PAI	399
C	READ IN SUBROUTINE COMMENTS	MAI	400
	REAC (5,25) (COMENT(J), J=1,14)	MAI	401
C	DECIDE WHICH SUBROUTINE IS CALLED	MAI	402
	IF (SUBNAME.EQ. SL1) GO TO 100	MAI	403
	IF (SUBNAME.EQ. SEC) GO TO 101	MAI	404
	IF (SUBNAME.EQ. VAN1) GO TO 102	MAI	405
	IF (SUBNAME.EQ. PCL) GO TO 103	MAI	406
	IF (SUBNAME.EQ. PIE) GO TO 106	MAI	407
	IF (SUBNAME.EQ. CUT) GO TO 107	MAI	408
	GO TO 99	MAI	409
100	CONTINUE	MAI	410
	REAC (5,400) PH11,XLMCA1,PH12,XLPDA2,TOLERD,NRAD	MAI	411
400	FORMAT (5F10.5,15)	MAI	412
	CALL SLICE (PH11,XLPDA1,PH12,XLPDA2,TOLERD,NRAD)	MAI	413
	GO TO 99	MAI	414
101	CONTINUE	MAI	415
	REAC (5,171) NSEC,NRAD	MAI	416
	CALL SECTNS(NSEC,NRAD)	MAI	417
	GO TO 99	MAI	418
102	CONTINUE	MAI	419
	REAC (5,202) NRAD,RPM,HMAP,WMAP	MAI	420
	CALL VANDER (RKM,HMAP,HMAP,NRAD)	MAI	421
	GO TO 99	MAI	422
103	CONTINUE	MAI	423
	REAC (5,202) NRAD,ANGPA,RKM	MAI	424
202	FORMAT (15,3F10.5)	MAI	425
	NPOLE=1	MAI	426
	CALL POLES (RKM,ANGPA,NRAD,NPOLE)	MAI	427
	NPOLE=2	MAI	428
	CALL POLES (RKM,ANGPA,NRAD,NPOLE)	MAI	429
	GO TO 99	MAI	430
106	CONTINUE	MAI	431
	REAC (5,44) R1,R2,TETA1,THETA2,XLMDA1,XLMDA2,NSPACE,NSLRF	MAI	432
44	FORMAT (6F10.5,215)	MAI	433
	CALL PIECE (R1,R2,TETA1,THETA2,XLMDA1,XLMDA2,NSPACE,NSLRF)	MAI	434
	GO TO 99	MAI	435
107	CONTINUE	MAI	436
	REAC (5,123) PH11,XLPDA1,PH12,XLPDA2,DEPTH1,DEPTH2	MAI	437
123	FORMAT (8F10.5)	MAI	438
	REAC (5,124) NCUT,NHCRZ,PMAGN1,ARCLNG,TOLERD	MAI	439
124	FORMAT (215,7F10.5)	MAI	440
	CALL CUTS (PH11,XLMDA1,PH12,XLMDA2,DEPTH1,DEPTH2,ARCLNG,TOLERD,	MAI	441
	NCUT,NHCRZ,PMAGN1)	MAI	442
99	CONTINUE	MAI	443
	STOP	MAI	444
	END	MAI	445
	SUBROUTINE CUTS (PH11,XLMDA1,PH12,XLMDA2,DEPTH1,DEPTH2,ARCLNG,	CUT	1
	TOLERD,NCUT,NHCRZ,PMAGN1)	CUT	2
C			


```

C
C
C      *CUTS*
C
C      FIND THE RELATIVE DENSITY, DENSITY, OR DENSITY VARIATION ON EACH
C      HORIZONTAL LINE
C      COMPUTE THE RELATIVE DENSITY, DENSITY, OR DENSITY VARIATION AT POINTS
C      THIS SUBROUTINE COMPUTES THE RELATIVE DENSITY, DENSITY, OR
C      DENSITY VARIATION ON VERTICAL RECTANGLES (CUTS) WHICH ARE
C      PERPENDICULAR TO A GREAT CIRCLE CONNECTING TWO POINTS ON THE EARTH'S
C      SURFACE AT INTERVALS EQUALLY SPACED ALONG THE GREAT CIRCLE SEGMENT.
C      HENCE WHEN LOOKING DOWN ON THE SURFACE OF THE EARTH IT LOOKS LIKE
C      THE LACINGS OF A FOOTBALL (WITH THE CUTS EXTENDING VERTICALLY
C      DOWNWARDS):
C
C
C
C      O      C      O      O
C      O      C      O      O
C      OXXXXXXOXXXXXXOXXXXXO
C      O      C      O      O
C      O      C      O      O
C
C      CUTS = 1 C
C      GREAT CIRCLE: X
C
C
C      EACH CUT IS DISPLAYED ALONG WITH THE TOPOGRAPHY ALONG THE TRACK
C      OF THE CUT.
C
C      ALL CUTS HAVE THE SAME LENGTH AND DEPTH. ALL POINTS ON A VERTICAL
C      PRINT-OUT (PHOTO) LINE HAVE THE SAME LATITUDE AND LONGITUDE.
C
C      THE CUTS ARE DISPLAYED AS RECTANGLES, SO THAT THERE IS A CERTAIN
C      AMOUNT OF DISTORTION. WE ARE LOOKING AT THE CUTS IN THE FOLLOWING
C      WAY: START WHERE THE GREAT CIRCLE INTERSECTS THE EQUATOR AND GO NORTH
C      ALONG THE GREAT CIRCLE UNTIL THE CUTS ARE REACHED.
C
C      THE TWO POINTS CONNECTED BY THE GREAT CIRCLE SEGMENT MAY BE
C      CHOSEN AT WILL. THE NUMBER OF CUTS, THEIR LENGTH, AND THEIR DEPTH MAY
C      ALSO BE CHOSEN AT WILL. THERE IS ALWAYS A CUT AT EACH ENDPOINT OF
C      THE GREAT CIRCLE SEGMENT.
C
C
C      NOTATION
C
C      PH11 = LATITUDE OF FIRST GREAT CIRCLE ENDPOINT IN DEGREES
C      XLMCA1 = LONGITUDE OF FIRST GREAT CIRCLE ENDPOINT IN DEGREES
C      PH12 = LATITUDE OF SECOND GREAT CIRCLE ENDPOINT IN DEGREES
C      XLMCA2 = LONGITUDE OF SECOND GREAT CIRCLE ENDPOINT IN DEGREES
C      DEPTH1 = DEPTH TO LOWER CUT BOUNDARY IN KILOMETERS
C      DEPTH2 = DEPTH TO UPPER CUT BOUNDARY IN KILOMETERS
C      ANGLNG = LENGTH OF CUT IN DEGREES
C      TOLEND = TOLERANCE LIMIT IN DEGREES, BELOW WHICH A SMALL
C      DIFFERENCE IN LATITUDE OR LONGITUDE OF THE GREAT CIRCLE
C      ENDPOINTS IS SET EQUAL TO ZERO TO AVOID SINGULARITIES
C      NCUT = NUMBER OF CUTS ALONG THE GREAT CIRCLE SEGMENT
C      NHORZ = LENGTH OF CUT IN SPACES ACROSS PAGE (OR PHOTO)
C      XPACAI = MAGNIFICATION OF DEPTH COMPARED TO LENGTH OF CUT (=1.0
C      FOR TRUE DEPTH TO LENGTH RATIO)
C
C
C      SUBROUTINES CALLED:
C
C      1. ANGLE
C      2. DENSITY
C      3. TOPCGR
C      4. VDG
C
C
C      NOTES
C
C      1. XLMCA1 .LE. XLMCA2.
C      2. DEPTH1 .GT. DEPTH2.
C      3. NHORZ IS ODD AND .LE. 121.
C      4. DEPTH1 IS USUALLY CHANGED SLIGHTLY BY THE SUBROUTINE TO MAKE
C      THE VERTICAL LENGTH OF THE CUTS AN INTEGER NUMBER OF SPACES
C      LONG ON THE PRINT-OUT PICTURE (OR DICED PHOTOGRAPH).
C      5. NCUT .GT. 1.
C
C
C      SAMPLE INPUT DATA (COLUMN 1 OF INPUT STARTS IN COLUMN 3 HERE)
C
C      SUBNAME (FORMAT: A6)
C      CUTS
C      (COMENT(J), J=1,14) (FORMAT: 13A6,A2)
C      TONGA TRENCH
C      PH11 XLMCA1 PH12 XLMCA2 DEPTH1 DEPTH2 (FORMAT:8F10.5)

```

```

C -23.44 125.11 -16.98 188.0 670.0 30.0 CUT 67
C NCUT=NCUT2 XMAGNI ARCLAG TOLERD (FORMAT: ',5,7F10.5) CUT 68
C 4 1C1 1.0 3C.C 0.0001 CUT 69
C
C IMPLICIT REAL*8(A-H,O-Z) CUT 70
C INTICER=2 TMAP(121), BETA(11) CUT 71
C DIMENSION ALPHA(23),LCW(1205,2) CUT 72
C DIMENSION XMAP(121) CUT 73
C DIMENSION XLP(2),PHI(2),PSI(2) CUT 74
C DIMENSION XLAT(121),XLONG(121),XGRID(121),YGRID(121) CUT 75
C DIMENSION COMENT(14) CUT 76
C DIMENSION IHTE(121) CUT 77
C COMMON/BLKA/XMAP CUT 78
C COMMON/BLKC/F,P1,P12,PICIV2,SCALE,NPHOTO,MAXSYM CUT 79
C COMMON/BLKD/ALPHA,LCW,1 CUT 80
C COMMON/BLKG/LMIN,LMAX,LLOW,LUP CUT 81
C COMMON/BLKH/RADAVG,RCR2,RLOWER,RUPPER CUT 82
C COMMON/BLKI/COMENT CUT 83
C COMMON/BLKJ/NDEG,REFDEN CUT 84
C COMMON/BLKT/BETA CUT 85
C DATA COT,EKS/IH.,IH)/ CUT 86
C
C P132=3.000*P1/2.000 CUT 87
C
C FIND MIDDLE OF SYMBOL/CCLER RANGE CUT 88
C SYMMAX=MAXSYM CUT 89
C SYMPL=SYMMAX/2.000 + C.500 CUT 90
C
C R1=1.000 - (DEPTH1/RADAVG) CUT 91
C R2=1.000 - (DEPTH2/RADAVG) CUT 92
C HCRZ=NHCRZ - 1 CUT 93
C XPICCL=(HCRZ/2.000) + 1.000 CUT 94
C MIDDLE=(NHCRZ - 1)/2 CUT 95
C STRECH=5.000/(4.000*XPMAGNI) CUT 96
C IF (NPHOTO .EQ. 1) STRECH=1.000/XMAGNI CUT 97
C FACTOR=HCRZ/(R2*ARCLNG*STRECH*F) CUT 98
C RY=(R2 - R1)*FACTOR + 1.000 CUT 99
C RY=RY CUT 100
C R1=R2 - RY/FACTOR CUT 101
C DEPTH1=RADAVG*(1.000 - R1) CUT 102
C ARCLNG=ARCLNG*(RADAVG/R2)*F CUT 103
C PRINT INPUT DATA CUT 104
C WRITE (6,78) CUT 105
C 78 FORMAT (I11) CUT 106
C WRITE (6,300) CUT 107
C 300 FORMAT (///,10X,'SURCUTLINE CALLED: CUTS',///) CUT 108
C WRITE (6,311) (COMENT(J), J=1,14) CUT 109
C 311 FORMAT (10X,13A6,2,///) CUT 110
C WRITE (6,47) PH11,XLMCA1 CUT 111
C 47 FORMAT (3X,'FIRST GREAT CIRCLE POINT: ',5X,'LATITUDE=',1X,F10.5, CUT 112
C . 1X,'DEGREES',10X,'LONGITUDE=',1X,F10.5,1X,'DEGREES',//) CUT 113
C WRITE (6,46) PH12,XLMCA2 CUT 114
C 46 FORMAT (3X,'SECOND GREAT CIRCLE POINT: ',5X,'LATITUDE=',1X,F10.5, CUT 115
C . 1X,'DEGREES',10X,'LONGITUDE=',1X,F10.5,1X,'DEGREES',//) CUT 116
C WRITE (6,45) DEPTH1,DEPTH2 CUT 117
C 45 FORMAT (5X,'DEPTHS BELOW SURFACE BETWEEN',1X,F10.5,1X,'KM AND',1X, CUT 118
C . F10.5,1X,'KM',//) CUT 119
C WRITE (6,48) NCUT,NHORZ,XMAGNI,ARCLNG,ARCKM CUT 120
C 48 FORMAT (5X,'NCUT=',15,1X,'NHORZ=',15,10X,'XMAGNI=',1X,F10.5,10X, CUT 121
C . 'ARCLNG=',1X,F10.5,1X,'DEGREES = ',F10.5,1X,'KM',//) CUT 122
C NCEG=1 CUT 123
C RADMAP=26.000 CUT 124
C WRITE (6,312) RADMAP CUT 125
C 312 FORMAT (///, 8X,'X,Y GRID COORDINATES ON VAN DER GRINTEN MAP WITH CUT 126
C .RADIUS',1X,F10.5,1X,'CM',//) CUT 127
C CALL VDG (PH11,XLPD1,RADMAP,NDEG,X,Y) CUT 128
C WRITE (6,313) X,Y CUT 129
C 313 FORMAT (10X,'FIRST GREAT CIRCLE POINT: ',3X,'XGRID=',1X,F8.3,1X, CUT 130
C . 'CM',10X,'YGRID=',1X,F8.3,1X,'CM',//) CUT 131
C CALL VDG (PH12,XLPD2,RADMAP,NDEG,X,Y) CUT 132
C WRITE (6,314) X,Y CUT 133
C 314 FORMAT (10X,'SECOND GREAT CIRCLE POINT: ',2X,'XGRID=',1X,F8.3,1X, CUT 134
C . 'CM',10X,'YGRID=',1X,F8.3,1X,'CM',//) CUT 135
C CONVERT ANGLES FROM DEGREES TO RADIAN CUT 136
C PH11=PH11*F CUT 137
C PH12=PH12*F CUT 138
C XLMCA1=XLMCA1*F CUT 139
C XLMCA2=XLMCA2*F CUT 140
C ARCLNG=ARCLNG*F CUT 141
C TOLER=TOLERD*F CUT 142
C FIND XXI, UMEGA, COSXXI, SINXXI, CCSOMG, SINOMG CUT 143
C TCLPHI=CSQRT(PH11**2 + PH12**2) CUT 144
C IS THE GREAT CIRCLE THE EQUATOR? CUT 145
C IF (TCLPHI - TOLER) 79,60,80 CUT 146
C 79 XXI=0.000 CUT 147

```

	CCSXXI=1.000	CUT	148
	SINXXI=C.000	CUT	149
	OMEGA=0.000	CUT	150
	CCSCPG=1.000	CUT	151
	SINCPG=C.000	CUT	152
	PSI(1)=XLMDA1	CUT	153
	PSI(2)=XLMDA2	CUT	154
	GC TC 01	CUT	155
80	TCLLAP=CABS(XLMDA2 - XLMDA1)	CUT	156
C	IS THE GREAT CIRCLE A MERIDIAN?	CUT	157
	IF (TCLLAP - TOLER) 82,83,83	CUT	158
82	XXI=PIDIV2	CUT	159
	CCSXXI=C.000	CUT	160
	SINXXI=1.000	CUT	161
	OMEGA=XLMDA1	CUT	162
	CCSCPG=CCOS(OMEGA)	CUT	163
	SINCPG=CSIN(OMEGA)	CUT	164
	PSI(1)=PHI1	CUT	165
	PSI(2)=PHI2	CUT	166
	GC TC 01	CUT	167
83	CONTINUE	CUT	168
	TANOPG=((DSIN(XLMDA1))*(DTAN(PHI2)) - (DSIN(XLMDA2))*(DTAN(PHI1)))/((CCS(XLMDA1))*(DTAN(PHI2)) - (DCOS(XLMDA2))*(DTAN(PHI1)))	CUT	169
	OMEGA=DATAN(TANOPG)	CUT	170
	TANXXI=(DTAN(PHI2))/(CSIN(XLMDA2 - OMEGA))	CUT	171
	IF (TANXXI) 52,52,53	CUT	172
52	OMEGA=OMEGA + PI	CUT	173
	TANXXI=-TANXXI	CUT	174
53	CONTINUE	CUT	175
	XXI=CATAN(TANXXI)	CUT	176
	IF (OMEGA) 55,54,54	CUT	177
55	OMEGA=OMEGA + PI2	CUT	178
54	CONTINUE	CUT	179
	CCSCPG=CCOS(OMEGA)	CUT	180
	SINCPG=DSIN(OMEGA)	CUT	181
	CCSXXI=CCOS(XXI)	CUT	182
	SINXXI=CSIN(XXI)	CUT	183
	PHI(1)=PHI1	CUT	184
	XLMDA(1)=XLMDA1	CUT	185
	PHI(2)=PHI2	CUT	186
	XLMDA(2)=XLMDA2	CUT	187
	DC 60 I=1,2	CUT	188
	B=XLMDA(1) - OMEGA	CUT	189
	IF (B) 56,57,57	CUT	190
56	B=B + PI2	CUT	191
57	CONTINUE	CUT	192
	CCSPS=(CCOS(B))*(CCS(PHI(1)))	CUT	193
	CCSPS=DABS(CCSPS)	CUT	194
	SINPS=DSQRT(1.000 - CCSPS**2)	CUT	195
	CALL ANGLE (CCSPS,SINPS,PS)	CUT	196
	IF (R - PI) 58,58,55	CUT	197
58	CONTINUE	CUT	198
	IF (R - PIV2) 64,64,61	CUT	199
64	PSI(1)=PS	CUT	200
	GC TC 60	CUT	201
61	PSI(1)=PI - PS	CUT	202
	GO TC 60	CUT	203
59	CONTINUE	CUT	204
	IF (R - PI2) 62,62,63	CUT	205
62	PSI(1)=PI + PS	CUT	206
	GC TC 60	CUT	207
63	PSI(1)=PI2 - PS	CUT	208
60	CONTINUE	CUT	209
81	CONTINUE	CUT	210
	OMEGAC=OMEGA/F	CUT	211
	XXIC=XXI/F	CUT	212
C	PRINT XXI AND OMEGA IN DEGREES	CUT	213
C	XXI = ANGLE OF GREAT CIRCLE WITH EQUATOR	CUT	214
C	OMEGA = LONGITUDE OF ASCENDING NODE OF GREAT CIRCLE, MEASURED	CUT	215
C	EASTWARD FROM GREENWICH	CUT	216
	WRITE (6,315)	CUT	217
315	FORMAT (////,8X,'GREAT CIRCLE LONGITUDE, INCLINATION TO EQUATOR,	CUT	218
	AND TOLERANCE 1',/)	CUT	219
	WRITE (6,77) OMEGAC,XXIC,TOLERO	CUT	220
77	FORMAT (9X,'OMEGA=',14,F10.5,1X,'DEGREES',10X,'XXI=',1X,F10.5,1X,	CUT	221
	'DEGREES',10X,'TOLERO=',1X,F15.10,1X,'DEGREES',/))	CUT	222
C	DPSI=PSI(2) - PSI(1)	CUT	223
	XNCUT=NCUT	CUT	224
	DLAPP=DPSI/(XNCUT - 1.000)	CUT	225
	CCSPSI=CCOS(PSI(1))	CUT	226
	SINPSI=CSIN(PSI(1))	CUT	227
	A11=CCSPSI*CCOSPG - CCSXXI*SINOPG*SINPSI	CUT	228
	A12=-SINPSI*CCOSPG - CCSXXI*SINOPG*CCSPSI	CUT	229
	A13=SINXXI*SINOPG	CUT	230
	A21=CCSPSI*SINOPG + CCSXXI*CCOSPG*SINPSI	CUT	231
	A22=-SINPSI*SINOPG + CCSXXI*CCOSPG*CCSPSI	CUT	232
	A23=-SINXXI*CCOSPG	CUT	233
		CUT	234

	A31=SINX1+SINPS1	CUT	235
	A32=SINX1*CCSPS1	CUT	236
	A33=CCSPX1	CUT	237
G	CC P6 J=1,121	CUT	238
	XLAT(J)=0.000	CUT	239
	XLONG(J)=0.000	CUT	240
#6	CONTINUE	CUT	241
C			
C			
	CC P5 I=1,NCLT	CUT	242
	X11=1 - 1	CUT	243
	WRITE (6,78)	CUT	244
	WRITE (6,71) 1	CUT	245
71	PCMPAT (77,7X,'CUT NUMBER = ',15,777)	CUT	246
	XLMPAD=X11*CLAMP	CUT	247
	CCSLPP=CCOSIXLMPAD	CUT	248
	SINLPP=CSINIXLMPAD	CUT	249
	CC P7 K=1,NHCRZ	CUT	250
	PK=K	CUT	251
	THETAP=PIDIV2 + (PK - XPICDL)*ANGLNO/NHCRZ	CUT	252
	CCS1P=CCOS(THETAP)	CUT	253
	SIN1P=CSIN(THETAP)	CUT	254
	XP=XS1P*CCSLPP	CUT	255
	YP=XS1P*SINLPP	CUT	256
	ZP=CCS1P	CUT	257
	X=A11*XP + A12*YP + A13*ZP	CUT	258
	Y=A21*XP + A22*YP + A23*ZP	CUT	259
	Z=A31*XP + A32*YP + A33*ZP	CUT	260
	XSQYSQ=CSQNT(X**2 + Y**2)	CUT	261
	IF (XSQYSQ) 66,67,66	CUT	262
67	PHIC=PIDIV2/F	CUT	263
	THETA=0.000	CUT	264
	IF (Z) 64,65,65	CUT	265
64	PHIC=PIDIV2/F	CUT	266
	THETA=PI	CUT	267
65	CONTINUE	CUT	268
	GO TO 68	CUT	269
66	U=7/XSQYSQ	CUT	270
	PHI=ATAN(U)	CUT	271
	THETA=PIDIV2 - PHI	CUT	272
	PHI=PHI/F	CUT	273
68	CONTINUE	CUT	274
	CALL ANGLE (X,Y,XLM(A)	CUT	275
	XLMPAD=XLMDA/F	CUT	276
	IF (XLMDAD) 73,74,74	CUT	277
73	XLMPAD=XLMDAD + 300.000	CUT	278
74	CONTINUE	CUT	279
	CALL TPCOR (THETA,XLMDA,H)	CUT	280
	INTC(K)=2.000*H + C.3DC + 23.000	CUT	281
	XLAT(K)=PHID	CUT	282
	XLONG(K)=XLMDAD	CUT	283
	CALL VDC (PHID,XLMDAD,HADMAP,NDEG,X,Y)	CUT	284
	XGRID(K)=X	CUT	285
	YGRID(K)=Y	CUT	286
87	CONTINUE	CUT	287
	WRITE (6,88)	CUT	288
88	FORPAT (1X,'POINT',3X,'LATITUDE',5X,'LONGITUDE',3X,'XGRID',5X,	CUT	289
	YGRID',11X,'POINT',3X,'LATITUDE',5X,'LONGITUDE',3X,'XGRID',5X,	CUT	290
	YGRID')	CUT	291
	WRITE (6,89)	CUT	292
89	FORPAT (1X,'(DEGREES)',4X,'(DEGREES)',4X,'(CM)',6X,'(CM)',19X,	CUT	293
	'(DEGREES)',4X,'(DEGREES)',4X,'(CM)',6X,'(CM)',77)	CUT	294
	CC P9 K=1,MICOLE	CUT	295
	KK=K + P100LE	CUT	296
	WRITE (6,91) K,XLAT(K),XLONG(K),XGRID(K),YGRID(K),KK,XLAT(KK),	CUT	297
	XLONG(KK),XGRID(KK),YGRID(KK)	CUT	298
91	FORPAT (2X,13,3X,F10.5,2X,F10.5,2X,F8.3,2X,F8.3,10X,13,3X,F10.5,	CUT	299
	3X,F10.5,2X,F8.3,2X,F8.3)	CUT	300
90	CONTINUE	CUT	301
	WRITE (6,92) NHCRZ,XLAT(NHCRZ),XLONG(NHCRZ),XGRID(NHCRZ),YGRID(NHCRZ)	CUT	302
	-RZ)	CUT	303
92	FORPAT (61X,13,3X,F10.5,3X,F10.5,2X,F8.3,2X,F8.3)	CUT	304
C	INITIALIZE LINE VALUES	CUT	305
C	XPAP IS FOR PRINT-OUT PICTURE	CUT	306
C	TPAP IS FOR DICOMED PICTURE	CUT	307
	CC 4 K=1,121	CUT	308
	TPAP(K) = BETA(11)	CUT	309
A	XPAP(K)=ALPHA(23)	CUT	310
	WRITE (6,78)	CUT	311
	WRITE (6,204)	CUT	312
204	FORPAT (4X,'KM',40X,'(DCTS INDICATE SEA LEVEL)',7)	CUT	313
	CC 201 LP=1,41	CUT	314
	LZ=42 - LP	CUT	315
	PLZ=LZ	CUT	316
	HEIGHT=(PLZ - 23.COC)/2.000	CUT	317
	CC 202 K=1,NHCRZ	CUT	318

IF (LZ .EQ. 23) XPAFI(K)=CUT	CUT	319
IF (INIT(K) .EQ. 17) XPAFI(K)=EKS	CUT	320
202 CONTINUE	CUT	321
WRITE (6,203) HEIGHT, (XPAFI(K), K=1,121)	CUT	322
203 PERMAT (1X,F5.1,12121)	CUT	323
CC 201 K=1,NCONZ	CUT	324
XPAFI(K)=ALPHA(23)	CUT	325
201 CONTINUE	CUT	326
NNY1=NNY + 1	CUT	327
C		
C FIND THE RELATIVE DENSITY, DENSITY, OR DENSITY VARIATION ON EACH	CUT	328
C HORIZONTAL LINE	CUT	329
CC 2 LP=1,NNY1	CUT	330
FLP1=LP - 1	CUT	331
R=R2 - FLP1/PACTOR	CUT	332
CC 3 K=1,NNHORIZ	CUT	333
C FIND THE X,Y,Z COORDINATES OF EACH POINT ON THE LINE	CUT	334
PR=K	CUT	335
THEIA=PI/180 + (FK - XPI00L)*ARCLNG/HORIZ	CUT	336
CCSTHP=PCOS(THETA)	CUT	337
SINTHP=CSIN(THETA)	CUT	338
XPR=X+SINTHP*CCSLMP	CUT	339
YPR=Y+SINTHP*CSLMP	CUT	340
ZPR=Z+CCSTHP	CUT	341
X=A11*XP + A12*YP + A13*ZP	CUT	342
Y=A21*XP + A22*YP + A23*ZP	CUT	343
Z=A31*XP + A32*YP + A33*ZP	CUT	344
C IS THE POINT IN THE CLRET	CUT	345
IF (R - RCONF) 26,21,27	CUT	346
26 JUMP=22	CUT	347
C IS USED FOR CONF	CUT	348
CC 10 24	CUT	349
27 CONTINUE	CUT	350
C IS THE POINT BELOW ELEMENT	CUT	351
IF (R - RLOWR) 101,102,102	CUT	352
101 CFN=0.000	CUT	353
CC 10 103	CUT	354
102 CONTINUE	CUT	355
C FIND THE SPHERICAL POLAR COORDINATES OF POINT	CUT	356
XSCYSC=CSQRT(X**2 + Y**2)	CUT	357
IF (Z) 24,25,24	CUT	358
25 THEIA=PI/180	CUT	359
CC 10 26	CUT	360
24 U=XSCYSC/Z	CUT	361
THEIA=ATAN(U)	CUT	362
IF (Z) 44,26,26	CUT	363
44 THETA=PI + THETA	CUT	364
26 CONTINUE	CUT	365
CALL ANGLE(X,Y,XLMD1)	CUT	366
C FIND THE RELATIVE DENSITY, DENSITY, OR DENSITY VARIATION AT POINT	CUT	367
CALL DENSITY (R,THETA,XLMDA,NDEN,REPOEN,DEN)	CUT	368
103 CONTINUE	CUT	369
C PUT THE RIGHT SYMBOL/NUMBER IN XPAFI(K)/TMAFI(K)	CUT	370
XS=(DEN/SCALE) + C.FOC	CUT	371
JNUP=SYML + XS	CUT	372
IF (JNUP .LE. 1) JNLP=1	CUT	373
IF (JNUP .GE. MAXSY) JNUP=MAXSY	CUT	374
29 XPAFI(K)=ALPHA(JNUP)	CUT	375
TMAFI(K) = BETA(JNUP)	CUT	376
3 CONTINUE	CUT	377
C PRINT THE LINE	CUT	378
WRITE (6,14) (XPAFI(K), K=1,121)	CUT	379
14 PERMAT (1X,121A1)	CUT	380
C WRITE (10,100)(TMAFI(K), K=1,121)	CUT	381
100 PERMAT (12112)	CUT	382
C RESET THE LINE	CUT	383
CC 15 K=1,121	CUT	384
XPAFI(K)=ALPHA(23)	CUT	385
TMAFI(K) = BETA(11)	CUT	386
15 CONTINUE	CUT	387
2 CONTINUE	CUT	388
65 CONTINUE	CUT	389
RETURN	CUT	390
END	CUT	391
SUBROUTINE PIECE (R1,R2,THETA1,THETA2,XLMDA1,XLMDA2,NSPACE,NSURF)	PIE	1
C		
C		
C *PIECE*	PIE	2
C		
C THIS SUBROUTINE COMPUTES THE RELATIVE DENSITY, DENSITY, OR	PIE	3
C DENSITY VARIATION ON A NUMBER OF SPHERICAL RECTANGLES, ALL WITH THE	PIE	4
C SAME ANGULAR COORDINATES BUT POSITIONED AT DIFFERENT DEPTHS.	PIE	5
C		
C A SPHERICAL RECTANGLE IS THE AREA ON THE SURFACE OF A SPHERE	PIE	6
C BOUNDED BY TWO FIXED LATITUDES AND TWO FIXED LONGITUDES.	PIE	7
C		
C SPHERICAL RECTANGLES ARE ALWAYS COMPUTED FOR RADIAL DISTANCES R1	PIE	8

```

C AND R2, WITH THE OTHERS (IF ANY) SANDWICHED IN BETWEEN THESE TWO. PIE 9
C THE SPHERICAL RECTANGLES ARE DISPLAYED AS RECTANGLES WITH THE PIE 10
C EAST-WEST DIRECTION RUNNING HORIZONTALLY ACROSS THE PAGE (PHOTO). SO PIE 11
C THERE IS A CERTAIN AMOUNT OF DISTORTION. PIE 12
C
C NOTATION PIE 13
C
C R1 = RADIAL DISTANCE OF LOWEST RECTANGLE IN KILOMETERS PIE 14
C R2 = RADIAL DISTANCE OF HIGHEST RECTANGLE IN KILOMETERS PIE 15
C THETA1 = COLATITUDE OF NORTHERN BOUNDARY OF THE RECTANGLES IN PIE 16
C DEGREES PIE 17
C THETA2 = COLATITUDE OF SOUTHERN BOUNDARY OF THE RECTANGLES IN PIE 18
C DEGREES PIE 19
C XLMDA1 = LONGITUDE OF THE WESTERN BOUNDARY OF THE RECTANGLES IN PIE 20
C DEGREES PIE 21
C XLMDA2 = LONGITUDE OF THE EASTERN BOUNDARY OF THE RECTANGLES IN PIE 22
C DEGREES PIE 23
C NSPACE = LENGTH OF THE NORTHERN AND SOUTHERN BOUNDARIES IN PIE 24
C HORIZONTAL SPACES ACROSS THE PAGE (PHOTO). PIE 25
C NSURF = NUMBER OF RECTANGLES DESIRED PIE 26
C
C SUBROUTINES CALLED: PIE 27
C
C 1. CENSTV PIE 28
C
C NOTES PIE 29
C
C 1. R2 .GT. R1. PIE 30
C 2. THETA2 .GT. THETA1. PIE 31
C 3. XLMDA2 .GT. XLMDA1. PIE 32
C 4. NSPACE .LE. 120. PIE 33
C 5. NSURF .GT. 1. PIE 34
C
C SAMPLE INPUT DATA (COLUMN 1 OF INPUT STARTS IN COLUMN 3 HERE) PIE 35
C
C SUBNAME (FORMAT: A6) PIE 36
C PIECE PIE 37
C (COPENT(J), J=1,14) (FORMAT: 13A6,A2) PIE 38
C HAWAII PIE 39
C
C R1 R2 THETA1 THETA2 XLMDA1 XLMDA2 NSPACE NSURF PIE 40
C (FORMAT: 6F10.5,2I5) PIE 41
C 2121.0 6321.0 50.0 80.0 180.0 210.0 80 3PIE 42
C
C IMPLICIT REAL*(A-H,O-Z) PIE 43
C INTEGER*2 THAP(121), BETA(11) PIE 44
C DIMENSION ALPHA(23),LCM(1205,2) PIE 45
C DIMENSION XMAP(121) PIE 46
C DIMENSION COPENT(14) PIE 47
C COMMON/BLKA/XMAP PIE 48
C COMMON/BLKC/F,PI,PI2,PICTV2,SCALE,NIPHOTO,MAXSYM PIE 49
C COMMON/BLKD/ALPHA,LCMH PIE 50
C COMMON/BLKG/LMIN,LMAX,LLON,LUP PIE 51
C COMMON/BLKH/RADAVG,PCRE,RLONER,NUPPER PIE 52
C COMMON/BLKI/CCHENT PIE 53
C COMMON/BLKJ/NDEN,REYDEN PIE 54
C COMMON/BLKT/BETA PIE 55
C
C PRINT INPUT DATA PIE 56
C WRITE (6,300) PIE 57
C 300 FORMAT (///,10X,'SUBROUTINE CALLED: PIECE',///) PIE 58
C WRITE (6,311) (COPENT(J), J=1,14) PIE 59
C 311 FORMAT (10X,13A6,A2,///) PIE 60
C
C FIND MIDDLE OF SYMREL/CCLER RANGE PIE 61
C SYMPAX=PAKSYM PIE 62
C SYMPL=SYMPAX/2.000 + C.500 PIE 63
C
C STRECH=5.000/4.000 PIE 64
C IF (NPHOTO .EQ. 1) STRECH=1.000 PIE 65
C
C WRITE (6,1) PIE 66
C 1 FORMAT (1H1) PIE 67
C NSP1=NSPACE + 1 PIE 68
C SURFCE=NSURF PIE 69
C SPACE=NSPACE PIE 70
C DR=(R2 - R1)/(SURFCE - 1.000) PIE 71
C DLMDA=(XLMDA2 - XLMDA1)/SPACE PIE 72
C DTHETA=CLMDA*STRECH PIE 73
C NTHETA=(THETA2 - THETA1)/DTHETA + 0.500000100 PIE 74

```

	TH=THETA	PIE	75
	NTH1=THETA + 1	PIE	76
	THETA2=THETA1 + TH*THETA	PIE	77
C	DR = DISTANCE BETWEEN SURFACES	PIE	78
C	DTHETA = LATITUDE DIFFERENCE BETWEEN NEIGHBORING POINTS	PIE	79
C	XLPCA = LONGITUDE DIFFERENCE BETWEEN NEIGHBORING POINTS	PIE	80
C			
	WRITE (6,2) R1,R2,DR	PIE	81
2	FORPAT (2X,'R1=',F10.3,1X,'KM',10X,'R2=',F10.3,1X,'KM',10X,'DR=',	PIE	82
	F10.3,1X,'KM',//)	PIE	83
	WRITE (6,3) THETA1,THETA2,DTHETA	PIE	84
3	FORPAT (2X,'THETA1=',F10.4,1X,'DEGREES',10X,'THETA2=',F10.4,1X,	PIE	85
	'DEGREES',10X,'DTHETA=',F10.4,1X,'DEGREES',//)	PIE	86
	WRITE (6,5) XLPCA1,DLPCA2,DLPCA	PIE	87
5	FORPAT (2X,'XLPCA1=',F10.4,1X,'DEGREES',10X,'XLPCA2=',F10.4,1X,	PIE	88
	'DEGREES',10X,'DLPCA=',F10.4,1X,'DEGREES',//)	PIE	89
C			
C	NORMALIZE DISTANCES TO EARTH RADIUS	PIE	90
	R1=R1/RADAVG	PIE	91
	R2=R2/RADAVG	PIE	92
	DR=DR/RADAVG	PIE	93
C	CONVERT ANGLES FROM DEGREES TO RADIANS	PIE	94
	THETA1=THETA1*F	PIE	95
	THETA2=THETA2*F	PIE	96
	DTHETA=DTHETA*F	PIE	97
	XLPCA1=XLPCA1*F	PIE	98
	XLPCA2=XLPCA2*F	PIE	99
	DLPCA=DLPCA*F	PIE	100
C			
	WRITE (6,1)	PIE	101
C			
C	INITIALIZE LINE VALUES	PIE	102
C	XMAP IS FOR PRINT-OUT PICTURE	PIE	103
C	TMAP IS FOR DICED PLOT	PIE	104
	DO 4 K=1,121	PIE	105
	TMAP(K)=BETA(11)	PIE	106
	XMAP(K)=ALPHA(12)	PIE	107
4			
C			
	R=R2 + DR	PIE	108
C			
	DO 10 ISURF=1,NSURF	PIE	109
	R=R - DR	PIE	110
	THETA=THETA1 + DTHETA	PIE	111
	DO 9 ITHETA=1,NTH1	PIE	112
	THETA=THETA + DTHETA	PIE	113
	XLPCA=XLPCA1 - DLPCA	PIE	114
	DO 6 K=1,NSP1	PIE	115
	XLPCA=XLPCA + DLPCA	PIE	116
C	COMPUTE THE RELATIVE DENSITY, DENSITY, OR DENSITY VARIATION AT POINT	PIE	117
	CALL DENSITY (R,THETA,XLPCA,NDEN,RLDEN,DEN)	PIE	118
C	PUT THE RIGHT SYMBOL/NUMBER IN XMAP(K)/TMAP(K)	PIE	119
	XS=(DEN/SCALE) + C.SDC	PIE	120
	JNUM=SYMBL + XS	PIE	121
	IF (JNUM .LE. 1) JNUM=1	PIE	122
	IF (JNUM .GE. MAXSYF) JNUM=MAXSYF	PIE	123
29	XMAP(K)=ALPHA(JNUM)	PIE	124
	TMAP(K) = BETA(JNUM)	PIE	125
8	CONTINUE	PIE	126
C	PRINT THE LINE	PIE	127
	WRITE (6,14) (XMAP(K), K=1,121)	PIE	128
14	FORPAT (5X,121A1)	PIE	129
C	WRITE (10,100) (TMAP(K), K=1,121)	PIE	130
C	FORPAT (121I2)	PIE	131
9	CONTINUE	PIE	132
	WRITE (6,1)	PIE	133
10	CONTINUE	PIE	134
	RETURN	PIE	135
	END	PIE	136
	SUBROUTINE PCLES (RPM,ANGMAX,NRAD,NPOLE)	POL	1
C			
C	*PCLES*	POL	2
C			
C	THIS SUBROUTINE COMPUTES THE RELATIVE DENSITY, DENSITY, OR	POL	3
C	DENSITY VARIATION ON A SURFACE OF CHOSEN RADIUS USING THE POLAR	POL	4
C	CARTHOGRAPHIC PROJECTION.	POL	5
C			
C	IT DISPLAYS THE NORTH POLAR REGION IF NPOLE=1 AND THE SOUTH	POL	6
C	POLAR REGION IF NPOLE=2.	POL	7
C			
C	NOTATION	POL	8
C			
C	RKM = RADIAL DISTANCE OF MAP SURFACE IN KILOMETERS	POL	9
C	ANGMAX = ANGULAR DISTANCE FROM PCLE TO MAP PERIMETER IN DEGREES	POL	10
C	NRAD = RADIUS OF THE MAP IN HORIZONTAL SPACES ACROSS THE PAGE	POL	11
C	(PHOTO)	POL	12
C	NPOLE = 1 FOR NORTH POLAR MAP; *2 FOR SOUTH POLAR MAP	POL	13
C			

C	SUBROUTINES CALLED:	POL	14
C	1. ANGLE	PCL	15
C	2. CIRC	PCL	16
C	3. DENSITY	PCL	17
C	NOTES	PCL	18
C	1. ANCMAX .LT. 9C DEGREES.	PCL	19
C	2. NRAC .LE. 6C.	PCL	20
C	SAMPLE INPUT DATA (COLUMN 1 OF INPUT STARTS IN COLUMN 3 HERE)	POL	21
C	SUBNAME (FORMAT: A6)	POL	22
C	POLES	PCL	23
C	(COMMENT(J), J=1,14) (FORMAT: 13A6,A2)	POL	24
C	SURFACE DENSITY DISTRIBUTION	PCL	25
C	NRAD ANCMAX RKM (FORMAT: 15,3F10.5)	POL	26
C	34 5C.0 6371.C	PCL	27
C	IMPLICIT REAL*8(A-H,O-Z)	POL	28
C	INTEGER*2 TMAP(121), BETA(11)	PCL	29
C	DIMENSION ALPHA(23),LCMF(1205,2)	PCL	30
C	DIMENSION XMAP(121)	PCL	31
C	DIMENSION COMMENT(14)	PCL	32
C	COMMON/BLKA/XMAP	PCL	33
C	COMMON/BLKG/F,P1,P12,PICIV2,SCALE,NPHOTO,MAXSYM	PCL	34
C	COMMON/BLKD/ALPHA,LCMFI	PCL	35
C	COMMON/BLKH/LMIN,LMAX,LLON,LUP	PCL	36
C	COMMON/BLKH/RADAVG,FCCRE,RLOWER,RUPPER	PCL	37
C	COMMON/BLKI/COMMENT	PCL	38
C	COMMON/BLKJ/NDEN,REFDEN	PCL	39
C	COMMON/BLKT/BETA	PCL	40
C	PRINT INPUT DATA	POL	41
C	WRITE (6,16)	PCL	42
C	WRITE (6,300)	PCL	43
300	FORMAT (///,10X,'SUBROUTINE CALLED: POLES',///)	PCL	44
C	WRITE (6,311) (COMMENT(J), J=1,14)	PCL	45
311	FORMAT (10X,13A6,A2,///)	PCL	46
C	WRITE (6,301) RKM	PCL	47
301	FORMAT (10X,'RKM =',1X,F10.3,1X,'KM',10X,'(RADIAL DISTANCE OF SURF	PCL	48
C	ACE)',///)	PCL	49
C	WRITE (6,302) NRAD	PCL	50
302	FORMAT (10X,'NRAD =',1X,14,10X,'(RADIUS OF MAP IN HORIZONTAL SPACE	PCL	51
C	S)',///)	PCL	52
C	WRITE (6,303) ANCMAX	PCL	53
303	FORMAT (10X,'ANCMAX =',1X,F10.5,1X,'DEGREES',10X,'(MAXIMUM COLATIT	PCL	54
C	UDE)',///)	PCL	55
C	R=RKM/RADAVG	PCL	56
C	ANG=ANCMAX*F	PCL	57
C	SANG=CSIN(ANG)	PCL	58
C	FIND MIDDLE OF SYMBOL/CCLER RANGE	POL	59
C	SYMPAX=MAXSYM	PCL	60
C	SYMBL=SYMPAX/2.0DC + C.000	PCL	61
C	COMPUTE NUMBER OF HORIZONTAL LINES IN MAP	POL	62
C	NRDSEC=NRAD	PCL	63
C	RDCSEC=NRAD	PCL	64
C	NRV=4*NRDSEC/5	PCL	65
C	IF (APHCTO .EQ. 1) ARV=NRDSEC	PCL	66
C	NRV=2*NRV + 1	PCL	67
C	NRV1=NRV + 1	PCL	68
C	NRV1=NRV1	PCL	69
CC	FIND LEFT AND RIGHT LIMITS OF MAP BY CALLING CIRC	POL	70
C	CALL CIRC(NRDSEC)	PCL	71
C	DO 10 NUPMAP=1,1	POL	72
C	INITIALIZE LINE VALUES	POL	73
C	XMAP IS FOR PRINT-OUT PICTURE	PCL	74
C	TMAP IS FOR DICOMED PHOTO	PCL	75
C	DO 4 K=1,121	PCL	76
C	TMAP(K) = BETA(11)	PCL	77
4	XMAP(K)=ALPHA(23)	PCL	78
C	WRITE (6,16)	POL	79
16	FORMAT (1H)	PCL	80
C	IF (NPOLE .EQ. 1) WRITE (6,30)	PCL	81

C	2. CIRC	SEC	18
C	3. CENSTY	SEC	19
C			
C	NTES	SEC	20
C			
C	1. NSEC IS CDC.	SEC	21
C	2. NRAD .LE. 6C.	SEC	22
C			
C	SAMPLE INPUT DATA (CCLLMN 1 OF INPUT STARTS IN COLUMN 3 HERE)	SEC	23
C	SUBNAME	(FORMAT: A)	SEC 24
C	SECTNS		SEC 25
C	(COPENT(J), J=1,14)	(FORMAT: 13A6,A2)	SEC 26
C	FIVE SECTIONS C-CSEN		SEC 27
C			
C	NSEC NRAD	(FORMAT: 4I5)	SEC 28
C	5 6C		SEC 29
C			
C	IMPLICIT REAL*8(A-H,O-Z)	SEC	30
C	INTEGER*2 TPAP(121), BETA(11)	SEC	31
C	DIMENSION ALPHA(23),LCWH(1205,2)	SEC	32
C	DIMENSION XPAP(121)	SEC	33
C	DIMENSION CCMPT(14)	SEC	34
C	CCMPCN/BLKA/XPAP	SEC	35
C	CCMPCN/PLKC/F,P1,P12,PICIV2,SCALE,NPHOTO,MAXSYM	SEC	36
C	CCMPCN/BLKD/ALPHA,LCWH	SEC	37
C	CCMPCN/BLKG/LPIN,LPXK,LLOW,LUP	SEC	38
C	CCMPCN/BLKH/RADAVC,PCRE,RLCHER,RUPPER	SEC	39
C	CCMPCN/BLKI/CCMPT	SEC	40
C	CCMPCN/BLKJ/NGEN,REFDEN	SEC	41
C	CCMPCN/BLKT/BETA	SEC	42
C			
C	PRINT INPLY DATA	SEC	43
C	WRITE (2,16)	SEC	44
C	WRITE (2,300)	SEC	45
C	3C0 FCRMAT (///,10X,'SUERCUTINE CALLED: SECTNS',///)	SEC	46
C	WRITE (6,311) (COPENT(J), J=1,14)	SEC	47
C	311 FCRMAT (10X,13A6,A2,///)	SEC	48
C	WRITE (6,301) NSEC	SEC	49
C	3C1 FCRMAT (10X,'NSEC =',1X,14,10X,'(NUMBER OF SECTIONS)',///)	SEC	50
C	WRITE (6,302) NRAD	SEC	51
C	3C2 FCRMAT (10X,'NRAD =',1X,14,10X,'(RADIUS OF EQUATOR IN HCRIZONTAL	SEC	52
C	'PACES)',///)	SEC	53
C			
C	FIND PICOLE OF SYMBOL/CCLCR RANGE	SEC	54
C	SYPMAX=MAXSYM	SEC	55
C	SYMBL=SYPMAX/2.CDC + C.5DO	SEC	56
C			
C	NHEM1=(NSEC - 1)/2 + 1	SEC	57
C	FRAD=NRAD	SEC	58
C	HEM1=NHEM1	SEC	59
C			
C	DO EACH SECTION	SEC	60
C	DO 1C JJ=1,NSEC	SEC	61
C	FJJ=NHEM1 - JJ	SEC	62
C	IF (JJ .EQ. NHEM1) GO TO 21	SEC	63
C	SQUARE=(FXAD**2)*(1.0C0 - (FJJ**2)/(HEM1**2))	SEC	64
C	RADSEC=CSQRT(SQUARE)	SEC	65
C	ZR=FRAD*(FJJ/HEM1)	SEC	66
C	NRDSEC=NRDSEC	SEC	67
C	RADSEC=NRDSEC	SEC	68
C	GC TC 22	SEC	69
C	21 NRDSEC=NRAD	SEC	70
C	THETA=PI/DIV2	SEC	71
C	RADSEC=FRAD	SEC	72
C			
C	22 CCNTINUE	SEC	73
C	CCMPUTE NUMBER OF HCRIZNTIAL LINES IN MAP	SEC	74
C	NRV=4*NRDSEC/5	SEC	75
C	IF (NPHOTO .EQ. 1) NRV=NRDSEC	SEC	76
C	NRV=2*NRV + 1	SEC	77
C	NRV1=NRV + 1	SEC	78
C	RV1=NRV1	SEC	79
C	FIND LEFT AND RIGHT LIMITS OF MAP BY CALLING CIRC	SEC	80
C	CALL CIRC(NRDSEC)	SEC	81
C			
C	INITIALIZE LINE VALUES	SEC	82
C	XPAP IS FOR PRINT-OUT PICTURE	SEC	83
C	TPAP IS FOR DICOMED PHOTO	SEC	84
C	DO 4 K=1,121	SEC	85
C	TPAP(K) = BETA(11)	SEC	86
C	XPAP(K)=ALPHA(23)	SEC	87
C			
C	SPACE CCMA THE PAGE	SEC	88

16	WRITE (6,16)	SEC	89
	FCMPAT (111)	SEC	90
	NSPACE=128 - NRY	SEC	91
	DC 17 KK=1,NSPACE	SEC	92
17	WRITE (6,18) ALPHA(23)	SEC	93
18	FCRMPAT (10X,1A1)	SEC	94
C	Z=FJJ*RLPPER/HEM1	SEC	95
C	FIND THE RELATIVE DENSITY, DENSITY, OR DENSITY VARIATION ON EACH	SEC	96
C	HORIZONTAL LINE	SEC	97
	DC 2 LP=1,NY	SEC	98
C	FIND THE X,Y,Z COORDINATES OF EACH POINT ON THE LINE	SEC	99
	LZ=NY - LP + 1	SEC	100
	FLZ=LZ	SEC	101
	STRECH=5.000/4.CDC	SEC	102
	IF (NPHCTO .EQ. 1) STRECH=1.000	SEC	103
	Y=(FLZ - RY1)*(STRECH*RLPPER)/RADSEC	SEC	104
	KMIN=LCWHI(LP,1)	SEC	105
	KMAX=LCWHI(LP,2)	SEC	106
	DC 3 K=KMIN,KMAX	SEC	107
	FK=K	SEC	108
	X=(FK - 61.000)*(RUPPER/MADSEC)	SEC	109
C	FIND THE SPHERICAL POLAR COORDINATES OF POINT	SEC	110
	R=DSQR(X**2 + Y**2 + Z**2)	SEC	111
C	IS THE POINT IN THE CIRCLE?	SEC	112
	IF (R - RCDRE) 20,27,27	SEC	113
20	JNUM=22	SEC	114
C	1 IS USED FOR CCHE	SEC	115
	GC 1C 29	SEC	116
27	CONTINUE	SEC	117
C	IS THE POINT BELOW RLCWER?	SEC	118
	IF (R - RLOWR) 1C1,1C2,102	SEC	119
1C1	DEN=C.CDC	SEC	120
	GC 1C 1C3	SEC	121
1C2	CONTINUE	SEC	122
	XSCYSC=DSQR(X**2 + Y**2)	SEC	123
	IF (Z) 24,25,24	SEC	124
25	THETA=PI/DIV2	SEC	125
	GC 1C 26	SEC	126
24	U=XSCYSC/Z	SEC	127
	THETA=DATAN(U)	SEC	128
	IF (Z) 44,26,26	SEC	129
44	THETA=PI + THETA	SEC	130
26	CONTINUE	SEC	131
	CALL ANGLE(X,Y,XLMDA)	SEC	132
C	COMPUTE THE RELATIVE DENSITY, DENSITY, OR DENSITY VARIATION AT POINT	SEC	133
	CALL DENSITY (R,THETA,XLMDA,NDEN,REFDEN,DEN)	SEC	134
1C3	CONTINUE	SEC	135
C	PUT THE RIGHT SYMBOL/NUMBER IN XMAP(K)/TMAP(K)	SEC	136
	XS=(DEN/SCALE) + C.SDC	SEC	137
	JNUM=SYMBL + XS	SEC	138
	IF (JNUM .LE. 1) JNUM=1	SEC	139
	IF (JNUM .GE. MAXSYB) JNUM=MAXSYB	SEC	140
29	XMAP(K)=ALPHA(JNUM)	SEC	141
	TMAP(K) = BETA(JNUM)	SEC	142
3	CONTINUE	SEC	143
C	PRINT THE LINE	SEC	144
	WRITE (6,14) (XMAP(K), N=1,121)	SEC	145
14	FCRMPAT (5X,121A1)	SEC	146
	WRITE(10,100)(TMAP(K), N=1,121)	SEC	147
100	FCRMPAT (12112)	SEC	148
C			
C	RESET THE LINE	SEC	149
	DC 15 K=KMIN,KMAX	SEC	150
	XMAP(K)=ALPHA(23)	SEC	151
	TMAP(K) = BETA(11)	SEC	152
15	CONTINUE	SEC	153
C			
2	CONTINUE	SEC	154
	XLAT=PI*(180.000/PI)	SEC	155
C	PRINT LATITUDE OF EACH SECTION	SEC	156
	WRITE (6,30) XLAT	SEC	157
30	FCRMPAT (///,90X,'LATITUDE=',F9.4,1X,'DEGREES')	SEC	158
1C	CONTINUE	SEC	159
	RETURN	SEC	160
	END	SEC	161
	SUBROUTINE SLICE (PHI1,XLMDA1,PHI2,XLMDA2,TOLRD,NRAD)	SLI	1
C			
C			
C	*SLICE*	SLI	2
C			
C	THIS SUBROUTINE COMPUTES THE RELATIVE DENSITY/DENSITY/DENSITY	SLI	3
C	VARIATION ON A PLANE WHICH PASSES THROUGH THE CENTER OF THE EARTH.	SLI	4
C			
C	THE INTERSECTION OF THE PLANE WITH THE EARTH IS CALLED A SLICE.	SLI	5
C			
C	THE SLICE IS ORIENTED SO AS TO CONTAIN THE TWO POINTS	SLI	6
C	(PHI1,XLMDA1) AND (PHI2,XLMDA2). THE LINE WHICH FORMS THE	SLI	7

```

C INTERSECTION OF THE SLICE WITH THE EQUATOR RUNS HORIZONTALLY ACROSS SLI 8
C THE PAGE (PHOTO). WE ARE LOOKING DOWN ON THE SLICE FROM THE NORTHERN SLI 9
C HEMISPHERE. SLI 10
C
C ACTATION SLI 11
C
C PH11 = LATITUDE OF FIRST POINT IN DEGREES SLI 12
C XLMCA1 = LONGITUDE OF FIRST POINT IN DEGREES SLI 13
C PH12 = LATITUDE OF SECOND POINT IN DEGREES SLI 14
C XLMCA2 = LONGITUDE OF SECOND POINT IN DEGREES SLI 15
C TOLERD = TOLERANCE LIMIT IN DEGREES, BELOW WHICH A SMALL SLI 16
C DIFFERENCE IN LATITUDE OR LONGITUDE OF THE TWO POINTS SLI 17
C IS SET EQUAL TO ZERO TO AVOID SINGULARITIES SLI 18
C NRAC = RADIUS OF SLICE IN HORIZONTAL SPACES ACROSS THE PAGE SLI 19
C (PHOTO) SLI 20
C
C SUBROUTINES CALLED: SLI 21
C
C 1. ANGLE SLI 22
C 2. CIRC SLI 23
C 3. DENSITY SLI 24
C 4. VCG SLI 25
C
C NOTES SLI 26
C
C 1. XLMCA2 .GT. XLMCA1. SLI 27
C 2. NRAC .LE. 60. SLI 28
C 3. SUBROUTINE CUTPLTS CARDS FOR CALCOMP PROGRAM. SLI 29
C
C SAMPLE INPUT DATA (COLUMN 1 OF INPUT STARTS IN COLUMN 3 HERE) SLI 30
C
C SUBNAME (FORMAT: A6) SLI 31
C SLICE SLI 32
C
C (COMENT(J), J=1,14) (FORMAT: 13A6,A2) SLI 33
C SLICE RUNS DOWN THE HAWAIIAN CHAIN FROM MIDWAY TO BIG ISLAND SLI 34
C
C PH11 XLMCA1 PH12 XLMCA2 TOLERD NRAC SLI 35
C (FORMAT: 5F10.5,15) SLI 36
C 28.11 183.35 15.24 206.59 0.0001 60 SLI 37
C
C
C IMPLICIT REAL*8(A-H,O/Z) SLI 38
C INTEGER*2 TMAP(121), RETA(11) SLI 39
C DIMENSION ALPHA(23),LCW(14205,2) SLI 40
C DIMENSION XMAP(121) SLI 41
C DIMENSION COMENT(14) SLI 42
C COMMON/BLKA/XMAP SLI 43
C COMMON/BLKC/F,P1,P12,PICLV2,SCALE,NPHOTO,MAXSYM SLI 44
C COMMON/BLKD/ALPHA,LCW1 SLI 45
C COMMON/BLKG/LMIN,LMAX,LLOW,LUP SLI 46
C COMMON/BLKH/RADAVG,FCCRE,RLCWER,RUPPER SLI 47
C COMMON/BLKI/COMENT SLI 48
C COMMON/BLKJ/ADEN,REFDEN SLI 49
C COMMON/BLKT/RETA SLI 50
C
C PRINT INPUT DATA SLI 51
C WRITE (6,16) SLI 52
C WRITE (6,300) SLI 53
C 300 FORMAT (///,10X,'SUBROUTINE CALLED: SLICE',///) SLI 54
C WRITE (6,311) (COMENT(J), J=1,14) SLI 55
C 311 FORMAT (10X,13A6,A2,///) SLI 56
C WRITE (6,47) PH11,XLMCA1 SLI 57
C 47 FORMAT (3X,'FIRST GREAT CIRCLE POINT:',5X,'LATITUDE=',1X,F10.5, SLI 58
C . 1X,'DEGREES',10X,'LONGITUDE=',1X,F10.5,1X,'DEGREES',///) SLI 59
C WRITE (6,46) PH12,XLMCA2 SLI 60
C 46 FORMAT (3X,'SECOND GREAT CIRCLE POINT:',5X,'LATITUDE=',1X,F10.5, SLI 61
C . 1X,'DEGREES',10X,'LONGITUDE=',1X,F10.5,1X,'DEGREES',///) SLI 62
C CONVERT ANGLES FROM DEGREES TO RADIANS SLI 63
C PH11=PH11*F SLI 64
C PH12=PH12*F SLI 65
C XLMCA1=XLMCA1*F SLI 66
C XLMCA2=XLMCA2*F SLI 67
C TOLERD=TOLERD*F SLI 68
C FIND XXI, OMEGA, COSX1, SINX1, COSCMG, SINCMG SLI 69
C TCLPHI=CSQRT(PH11**2 + PH12**2) SLI 70
C IS THE GREAT CIRCLE THE EQUATOR? SLI 71
C IF (TCLPHI - TOLERD) 79,80,80 SLI 72
C 79 XXI=C.000 SLI 73
C COSX1=1.000 SLI 74
C SINX1=0.000 SLI 75
C OMEGA=0.000 SLI 76
C COSCMG=1.000 SLI 77

```

	SINCPG=C.000	SLI	78
	GC IC B1	SLI	79
HC	TCLLAP=CABS(XLMCA2 + XLPDA1)	SLI	80
C	IS THE GREAT CIRCLE A MERIDIAN?	SLI	81
	IF (TCLLAP - TCLER) 82,F3,B3	SLI	82
82	XX1=PIDIV2	SLI	83
	CCSP1=0.000	SLI	84
	SINX1=1.000	SLI	85
	OPECA=XLMDA1	SLI	86
	CCSCPG=CCOS(CMEGA)	SLI	87
	SINCPG=CSIN(CMEGA)	SLI	88
	GC IC B1	SLI	89
83	CCNTINUE	SLI	90
	TANCPG=((OSIN(XLMCA1))*(DTAN(PHI2)) - (OSIN(XLMCA2))*(DTAN(PHI1)))	SLI	91
	./((CCOS(XLMCA1))*(DTAN(PHI2)) - (CCOS(XLMCA2))*(DTAN(PHI1)))	SLI	92
	OPECA=CATAN(TANCPG)	SLI	93
	TANXX1=(DTAN(PHI2))/(CSIN(XLMCA2 - OMEGA))	SLI	94
	IF (TANXX1) 52,52,53	SLI	95
52	OPECA=OMEGA + PI	SLI	96
	TANXX1=-TANXX1	SLI	97
53	CCNTINUE	SLI	98
	XX1=CATAN(TANXX1)	SLI	99
	IF (CMEGA) 55,54,54	SLI	100
55	OPECA=OMEGA + PI2	SLI	101
54	CCNTINUE	SLI	102
	XXIC=XX1/F	SLI	103
	OPECAC=CMEGA/F	SLI	104
C	PRINT XX1 AND OMEGA IN DEGREES	SLI	105
C	XX1 = ANGLE OF GREAT CIRCLE WITH EQUATOR	SLI	106
C	OMEGA = LONGITUDE OF ASCENDING NODE OF GREAT CIRCLE, MEASURED	SLI	107
C	EASTWARD FROM GREENWICH	SLI	108
	WRITE (6,301) XXIC	SLI	109
301	FORMAT (10X,'XX1 =',1X,F10.5,1X,'DEGREES',10X,'(INCLINATION TO EQUATOR)',//)	SLI	110
	WRITE (6,303) OMEGAC	SLI	111
303	FORMAT (10X,'OMEGA =',1X,F10.5,1X,'DEGREES',10X,'(NODE MEASURED EAST FROM GREENWICH)',//)	SLI	112
C	PRINT ARAC	SLI	113
	WRITE (6,302) NRAC	SLI	114
302	FORMAT (10X,'NRAC =',1X,F4,10X,'(RADIUS OF SLICE IN HORIZONTAL SPACES)',//)	SLI	115
C		SLI	116
	CCSX1=CCOS(XX1)	SLI	117
	SINX1=OSIN(XX1)	SLI	118
	CCSCPG=CCOS(CMEGA)	SLI	119
	SINCPG=CSIN(CMEGA)	SLI	120
B1	CCNTINUE	SLI	121
C		SLI	122
C		SLI	123
C	CCPLTE CALCOMP PLOTTER DATA FOR PLOTTING TOPOGRAPHY OF SLICE	SLI	124
C	AND GREAT CIRCLE ON VAN DER GRINTEN MAP	SLI	125
C	RADPAF = RADIUS OF VAN DER GRINTEN MAP IN INCHES	SLI	126
	RADPAF=10.187500	SLI	127
C	CCNVER = INCH TO KM RATIO USED IN TOPOGRAPHY PLOT	SLI	128
	CCNVER=0.100	SLI	129
	RADSEC=NRAD	SLI	130
	RCIACH=RADSEC*(0.1DC)	SLI	131
	RINCH=RCINCH + 1.CDC	SLI	132
	NCEG=1	SLI	133
	WRITE (6,208)	SLI	134
208	FORMAT (//////,10X,'CALCOMP PLOT DATA',//)	SLI	135
	WRITE (6,204) RADPAF	SLI	136
204	FORMAT (12X,'RADIUS OF VAN DER GRINTEN MAP =',F7.3,1X,'INCHES')	SLI	137
	WRITE (6,205) CCNVER	SLI	138
205	FORMAT (//,12X,'INCHES PER KM OF TOPO HEIGHT =',F10.5)	SLI	139
	WRITE (6,16)	SLI	140
	WRITE (6,206)	SLI	141
206	FORMAT (2X,'K',7X,'FSI',7X,'LATITUDE',4X,'LONGITUDE',2X,'TOPO HEIGHT',4X,'XGRID',7X,'GRID',10X,'XH',10X,'YH')	SLI	142
	WRITE (6,207)	SLI	143
207	FORMAT (8X,'(DEGREES)',3X,'(DEGREES)',3X,'(DEGREES)',5X,'(KM)',4X,'(INCHES)',4X,'(INCHES)',5X,'(INCHES)',4X,'(INCHES)',//)	SLI	144
	DC 201 K=1,360	SLI	145
	PSIC=K - 1	SLI	146
	PSI=PSIC*F	SLI	147
	CCSPSI=CCOS(PSI)	SLI	148
	SINPSI=CSIN(PSI)	SLI	149
	X=CCSPSI*CCOSPG - CCSX1*SINMG*SINPSI	SLI	150
	Y=CCSPSI*SINCPG + CCSX1*CCOSPG*SINPSI	SLI	151
	Z=SINX1*SINPSI	SLI	152
	XSQYSC=CSQRT(X**2 + Y**2)	SLI	153
	IF (XSQYSC) 66,67,66	SLI	154
67	PHIC=PIDIV2/F	SLI	155
	THETA=0.000	SLI	156
	IF (Z) 84,85,85	SLI	157
84	PHIC=-PIDIV2/F	SLI	158
	THETA=PI	SLI	159
		SLI	160
		SLI	161

85	CONTINUE	SLI 162
	GC TC 60	SLI 163
66	U=Z/XSQYSG	SLI 164
	PHI=CATAN(U)	SLI 165
	THETA=PIDIVZ * PHI	SLI 166
	PHIC=PHI/F	SLI 167
68	CONTINUE	SLI 168
	CALL ANGLE (X,Y,XLPEA)	SLI 169
	XLPCAC=XLMDA/F	SLI 170
	IF (XLMDA) 73,74,74	SLI 171
73	XLPCAC=XLMDAC + 360.000	SLI 172
74	CONTINUE	SLI 173
	CALL TOPOGR (THETA,XLMDA,H)	SLI 174
	H=F*CCNVER	SLI 175
	CALL VDG (PHIC,XLMDA,D,RADMAP,NDEG,XG,YG)	SLI 176
	XH=(IRINCH + H)*CCSF51	SLI 177
	YH=(IRINCH + H)*SINF51	SLI 178
202	FCRMAP (1X,14,6(2X,F1C.2),3X,F10.3,2X,F1C.3)	SLI 179
	WRITE (6,202) K,PSIL,PHID,XLMDA,H,XG,YG,XH,YH	SLI 180
	WRITE (7,203) K,XC,YC,XF,YH	SLI 181
203	FCRMAP (15,4F10.3)	SLI 182
201	CONTINUE	SLI 183
C		
C		
C		
C	FIND MIDDLE OF SYMBOL/CCLER RANGE	SLI 184
	SYMPAX=MAXSYM	SLI 185
	SYMPRL=SYMPAX/2.CDC + C.200	SLI 186
C		
C	COMPUTE NUMBER OF HORIZINTIAL LINES IN MAP	SLI 187
	NROSEC=NRAD	SLI 188
	RADSEC=NRAD	SLI 189
	NRV=4*NROSEC/5	SLI 190
	IF (INPHCTO .EQ. 1) NRV=NROSEC	SLI 191
	NRV=2*NRV + 1	SLI 192
	NRV1=NRV + 1	SLI 193
	RV1=NRV1	SLI 194
C	FIND LEFT AND RIGHT LIMITS OF MAP BY CALLING CIRC	SLI 195
	CALL CIRCINROSEC	SLI 196
C		
	DC 10 NUPMAP=1,1	SLI 197
C		
C	INITIALIZE LINE VALUES	SLI 198
C	XMAP IS FOR PRINT-OUT PICTURE	SLI 199
C	TMAP IS FOR DICOMED PHOTO	SLI 200
	DC 4 K=1,121	SLI 201
	TMAP(K) = BETA(11)	SLI 202
4	XMAP(K)=ALPHA(23)	SLI 203
C		
C	SPACE DOWN THE PAGE	SLI 204
	WRITE (6,16)	SLI 205
16	FCRMAP (1H1)	SLI 206
	NSPACE=120 - NRV	SLI 207
	DC 17 KM=1,NSPACE	SLI 208
17	WRITE (6,18) ALPHA(23)	SLI 209
18	FCRMAP (10X,1A1)	SLI 210
C		
C	FIND THE RELATIVE DENSITY, DENSITY, OR DENSITY VARIATION ON EACH	SLI 211
C	HORIZINTIAL LINE	SLI 212
	DC 2 LP=1,NV	SLI 213
	LZ=NV - LP + 1	SLI 214
	FLZ=LZ	SLI 215
	KMIN=LOWHI(LP,1)	SLI 216
	KMAX=LOWHI(LP,2)	SLI 217
C		
	DC 3 K=KMIN,KMAX	SLI 218
C	FIND THE X,Y,Z COORDINATES OF EACH POINT ON THE LINE	SLI 219
	FK=K	SLI 220
	XP=(FK - 61.000)*(RLPPER/RADSEC)	SLI 221
	STRECH=5.000/4.000	SLI 222
	IF (INPHCTO .EQ. 1) STRECH=1.000	SLI 223
	YP=(FLZ - RV1)*(STRECH*RLPPER)/RADSEC	SLI 224
	X=(CCSOMG)*XP - (COSX1*(SINOMG)*YP	SLI 225
	Y=(SINOMG)*XP + (COSX1*(COSOMG)*YP	SLI 226
	Z=(SINX1)*YP	SLI 227
C	FIND THE SPHERICAL POLAR COORDINATES OF POINT	SLI 228
	R=DSCHT(XP**2 + YP**2)	SLI 229
C	IS THE POINT IN THE CORE?	SLI 230
	IF (R - RCORE) 28,27,27	SLI 231
28	JNUP=22	SLI 232
C	8 IS USED FOR CORE	SLI 233
	GC TC 29	SLI 234
27	CONTINUE	SLI 235
C	IS THE POINT BELOW RLCEWET?	SLI 236
	IF (R - RLOWER) 101,102,102	SLI 237
101	DEN=C.000	SLI 238
	GC TC 103	SLI 239

102	CONTINUE	SLI	240
	XSQVSC=ESQRT(X**2 + Y**2)	SLI	241
	IF (Z) 24,25,24	SLI	242
25	THETA=PIDIV2	SLI	243
	GO TO 26	SLI	244
24	U=XSCVSC/Z	SLI	245
	THETA=CATAN(U)	SLI	246
	IF (Z) 44,26,26	SLI	247
44	THETA=PI + THETA	SLI	248
26	CONTINUE	SLI	249
	CALL ANGLE(X,Y,XLPD)	SLI	250
C	COMPUTE THE RELATIVE DENSITY, DENSITY, OR DENSITY VARIATION AT POINT	SLI	251
	CALL CENSTY (X,THETA,XLPD,NDEN,REFDEN,DEN)	SLI	252
103	CONTINUE	SLI	253
C	PUT THE RIGHT SYMBOL/NUMBER IN XMAP(K)/TMAP(K)	SLI	254
	XS=(DEN/SCALE) * C.SDC	SLI	255
	JNUP=SYMBL * XS	SLI	256
	IF (JNUP .LE. 1) JNLM=1	SLI	257
	IF (JNUP .GE. MAXSYM) JNUP=MAXSYM	SLI	258
29	XMAP(K)=ALPHA(JNUP)	SLI	259
	TMAP(K) = BETA(JNLM)	SLI	260
3	CONTINUE	SLI	261
C	PRINT THE LINE	SLI	262
	WRITE (6,14) (XMAP(I), K=1,121)	SLI	263
14	FORMAT (5X,121A1)	SLI	264
C	WRITE (10,1001)(TMAP(K), K=1,121)	SLI	265
C 100	FORMAT (12112)	SLI	266
C	RESET THE LINE	SLI	267
	GO TO K=KMIN,KMAX	SLI	268
	XMAP(K)=ALPHA(23)	SLI	269
	TMAP(K) = BETA(11)	SLI	270
15	CONTINUE	SLI	271
2	CONTINUE	SLI	272
C	END	SLI	275
10	CONTINUE	SLI	273
	RETURN	SLI	274
	END	SLI	275
	SUBROUTINE VANDER (RKM,TMAP,WMAP,NRAD)	VAN	1
C			
C	*VANDER*	VAN	2
C			
C	THIS SUBROUTINE COMPUTES THE RELATIVE DENSITY, DENSITY, OR	VAN	3
C	DENSITY VARIATION ON A SURFACE OF CHOSEN RADIUS USING THE VAN DER	VAN	4
C	GRINTEN PROJECTION.	VAN	5
C			
C	IT DIVIDES THE MAP INTO TWO HEMISPHERES TO MAKE THE MAP BIG	VAN	6
C	ENOUGH TO OVERLAY ON PALL LCHMAN'S TECTONIC ACTIVITY MAP.	VAN	7
C			
C	NOTATION	VAN	8
C			
C	RKM = RADIAL DISTANCE OF MAP SURFACE IN KILOMETERS	VAN	9
C	HMAP = TOTAL HEIGHT OF OVERLAY MAP IN CENTIMETERS	VAN	10
C	WMAP = TOTAL WIDTH OF OVERLAY MAP IN CENTIMETERS	VAN	11
C	NRAD = RADIUS OF MAP IN HORIZONTAL SPACES ACROSS THE PAGE	VAN	12
C	(PHOTO)	VAN	13
C			
C	SUBROUTINES CALLED:	VAN	14
C			
C	1. CIRC	VAN	15
C	2. CUBIC	VAN	16
C	3. CENSTY	VAN	17
C	4. QUACRC	VAN	18
C			
C	NOTES	VAN	19
C			
C	1. NRAD .LE. 102.	VAN	20
C	2. WMAP .LE. 52 CM.	VAN	21
C			
C	SAMPLE INPUT DATA (COLUMN 1 OF INPUT STARTS IN COLUMN 3 HERE)	VAN	22
C			
C	SUBNAME (FORMAT: A6)	VAN	23
C	VANDER	VAN	24
C	(COMMENT(J), J=1,14) (FORMAT: 13A6,A2)	VAN	25
C	SURFACE MAP	VAN	26
C			
C	NRAD RKM HMAP WMAP (FORMAT: 15,3F10.5)	VAN	27
C	102 6371.0 38.2 52.0	VAN	28
C			
C	IMPLICIT REAL*8(A-H,O-Z)	VAN	29
C	INTEGER*2 TMAP(121), BETA(11)	VAN	30

	DIMENSION ALPHA(23),LCW(1209,2)	VAN	31
	DIMENSION XPAP(1211)	VAN	32
	DIMENSION CCMENT(14)	VAN	33
	CCPPCN/BLKA/XPAP	VAN	34
	CCPPCN/BLKC/F,P1,P12,P1CIV2,SCALE,NPHOTO,MAXSYM	VAN	35
	CCPPCN/BLKC/ALPHA,LCW1	VAN	36
	CCPPCN/BLKC/LPIN,LMAX,LLOW,LUP	VAN	37
	CCPPCN/BLKH/RADAVG,FCCRE,RLCHER,RUPPER	VAN	38
	CCPPCN/BLK1/CCPENT	VAN	39
	CCPPCN/BLKJ/NGEN,REIDEN	VAN	40
	CCPPCN/BLK1/BETA	VAN	41
C			
C	PRINT INPT DATA	VAN	42
	WRITE (6,16)	VAN	43
	WRITE (6,300)	VAN	44
300	FCRPAI (///,10X,'SUBROUTINE CALLED: VANDER',///)	VAN	45
	WRITE (6,311) (CCMENT(J), J=1,14)	VAN	46
311	FCRPAI (10X,13A6,A2,///)	VAN	47
	WRITE (6,301) RKM	VAN	48
301	FCRPAI (10X,'RKM =',1X,F10.3,1X,'KM',10X,'(RADIAL DISTANCE OF SUNF	VAN	49
	.AGE)',///)	VAN	50
	WRITE (6,302) NRAC	VAN	51
302	FCRPAI (10X,'NRAC =',1X,14,10X,'(RADIUS OF MAP IN HORIZONTAL SPACEVA	VAN	52
	.S)',///)	VAN	53
C			
	R=RKM/RADAVG	VAN	54
C			
C	FIND MIDDLE OF SYMBL/CCLER RANGE	VAN	55
	SYPMAX=MAXSYM	VAN	56
	SYMBL=SYPMAX/2.CDC + C.500	VAN	57
C			
C	COMPUTE NUMBER OF HORIZONTAL LINES IN MAP	VAN	58
	NROSEC=NRAC	VAN	59
	RADSEC=NRAC	VAN	60
	NRV=400NRROSEC/5	VAN	61
	IF (NPHOTO .EQ. 1) ARV=NRROSEC	VAN	62
	NRV=20NRV + 1	VAN	63
	NRV1=NRV + 1	VAN	64
	RV1=NRV1	VAN	65
C	FIND LEFT AND RIGHT LIMITS OF MAP BY CALLING CIRC	VAN	66
	CALL CIRC(NROSEC)	VAN	67
C			
	EE 10 NUPMAP=1,1	VAN	68
C			
C	DC WESTERN HEMISPHERE, THEN EASTERN HEMISPHERE	VAN	69
	DC 10 NHEMIS=1,2	VAN	70
C	INITIALIZE LINE VALUES	VAN	71
C	XPAP IS FOR PRINT-CLT PICTURE	VAN	72
C	TPAP IS FOR DICOPED PHOTO	VAN	73
	DC 4 K=1,121	VAN	74
	TPAP(K) = RETA(11)	VAN	75
	XPAP(K)=ALPHA(23)	VAN	76
C			
	WRITE (6,16)	VAN	77
16	FCRPAI (111)	VAN	78
	NV=(RV1 - 1.CDC)*XPAP/XPAP	VAN	79
	LPMIN=NRV - NV	VAN	80
	LPMAX=NRV - (LPMIN + 1)	VAN	81
C	FIND THE RELATIVE DENSITY, DENSITY, OR DENSITY VARIATION ON EACH	VAN	82
C	HORIZONTAL LINE	VAN	83
	DC 2 LP=LPMIN,LPMAX	VAN	84
	IF (NHEMIS .EQ. 2) GO TO 51	VAN	85
	TERM=C.CDC	VAN	86
	KPIN=1	VAN	87
	KMAX=LOWHI(LP,2) - 40	VAN	88
	GO TO 52	VAN	89
51	TERM=RACSEC	VAN	90
	KPIN=LOWHI(LP,1) - 40 + NROSEC	VAN	91
	KMAX=NRACSEC	VAN	92
52	CONTINUE	VAN	93
	LZ=NV - LP + 1	VAN	94
	FLZ=LZ	VAN	95
C			
	DC 3 K=KPIN,KMAX	VAN	96
C	FIND THE X,Y,Z COORDINATES OF EACH POINT ON THE LINE	VAN	97
	FK=K	VAN	98
	X=FK - 1.000 - TERM	VAN	99
	STRECH=5.000/4.000	VAN	100
	IF (NPHOTO .EQ. 1) STRECH=1.000	VAN	101
	Y=(FLZ - RV1)*STRECH	VAN	102
C	FIND THE SPHERICAL POLAR COORDINATES OF POINT	VAN	103
	CALL CUBIC(X,Y,RACSEC,TPETA)	VAN	104
	CALL CUADRCIX,Y,RADSEC,XLPOA)	VAN	105
C	COMPUTE THE RELATIVE DENSITY, DENSITY, OR DENSITY VARIATION AT POINT	VAN	106
	CALL DENSITY (R,THETA,XLPOA,NGEN,REIDEN,DEN)	VAN	107
C	PUT THE RIGHT SYMBOL/NUMBER IN XPAP(K)/TPAP(K)	VAN	108
	XS=(DEN/SCALE) + C.500	VAN	109
	XNUP=SYMBL + XS	VAN	110

	IF (JNUP .LE. 1) JNUP=1	VAN	111
	IF (JNUP .GE. MAXSYM) JNUP=MAXSYM	VAN	112
29	XMAP(K)=ALPHA(JNUP)	VAN	113
	THAP(K) = BETA(JNUP)	VAN	114
3	CONTINUE	VAN	115
C	PRINT THE LINE	VAN	116
	WRITE (6,14) (XMAP(K), K=1,121)	VAN	117
14	FCRPA1 (5X,121A1)	VAN	118
C	WRITE (10,100) (THAP(K), K=1,121)	VAN	119
C 100	FCRPA1 (121I2)	VAN	120
C			
C	RESET THE LINE	VAN	121
	DO 15 K=KMIN,KMAX	VAN	122
	XMAP(K)=ALPHA(123)	VAN	123
	THAP(K) = BETA(11)	VAN	124
15	CONTINUE	VAN	125
C			
2	CONTINUE	VAN	126
C			
10	CONTINUE	VAN	127
	RETLN	VAN	128
	END	VAN	129
	SUBROUTINE DENSITY (F,THETA,XLPDA,NDEN,REFDEN,DEN)	DEN	1
C			
C	THIS SUBROUTINE COMPUTES THE RELATIVE DENSITY, DENSITY, OR	DEN	2
C	DENSITY VARIATION AT A POINT INSIDE THE EARTH.	DEN	3
C			
C			
C	ACIATION	DEN	4
C			
C	R = RADIAL DISTANCE OF POINT FROM THE CENTER OF THE EARTH,	DEN	5
C	NORMALIZED TO THE EARTH'S RADIUS	DEN	6
C	THETA = COLATITUDE OF POINT IN RADIANS	DEN	7
C	XLPDA = ANGLE OF POINT WITH THE X-AXIS, LYING IN THE X-Y PLANE,	DEN	8
C	MEASURED IN RADIANS	DEN	9
C	DEN = RELATIVE DENSITY, DENSITY, OR DENSITY VARIATION AT THE	DEN	10
C	POINT	DEN	11
C	NDEN = 0 FOR RELATIVE DENSITY, =1 FOR ACTUAL DENSITY,	DEN	12
C	=2 FOR DENSITY VARIATION	DEN	13
C			
C	SUBROUTINES CALLED:	DEN	14
C			
C	1. LGENDR	DEN	15
C	2. CZIEN (IF NDEN=1 OR NDEN=2)	DEN	16
C			
C	IMPLICIT REAL*8(A-H,O-Z)	DEN	17
	DIMENSION CLM(36,37,2),COE(36)	DEN	18
	DIMENSION PBAR(103)	DEN	19
	COMMON/BLKB/CLM,CCE	DEN	20
	COMMON/BLKB/F,PI,PI2,PI2V2,SCALE,NPHOTO,MAXSYM	DEN	21
	COMMON/BLKB/LMIN,LMAX,LLOW,LUP	DEN	22
	COMMON/BLKB/RADAVG,PCCRE,RLOWER,RUPPER	DEN	23
	COMMON/BLKB/PBAR	DEN	24
C	CHANGE VARIABLES FROM THETA TO PHI	DEN	25
	PI=PI2V2 - THETA	DEN	26
C	COMPUTE LEGENDRE POLYNOMIALS	DEN	27
	CALL LGENDR(PHI,LPA)	DEN	28
C	COMPUTE RELATIVE DENSITY	DEN	29
	SUM=C.OO	DEN	30
	DO 5 L=LMIN,LMAX	DEN	31
	RL=R*OL	DEN	32
	MAX=L + 1	DEN	33
	DO 5 M=1,MAX	DEN	34
	XP=M - 1	DEN	35
	ARG=XP*XLMDA	DEN	36
	SS=CSIN(ARG)	DEN	37
	CC=CCCS(ARG)	DEN	38
	IND=M + L*(L+1)/2	DEN	39
	SUM=SUM + (CLM(L,M,1)*CC + CLM(L,M,2)*SS)*(PBAR(IND))*RL	DEN	40
5	CONTINUE	DEN	41
	DEN=SUM	DEN	42
C	SEE IF ACTUAL DENSITY IS WANTED	DEN	43
	IF (NDEN .EQ. 1) GO TO 7	DEN	44
C	SEE IF DENSITY VARIATION IS WANTED	DEN	45
	IF (NDEN .EQ. 2) GO TO 5	DEN	46
	GO TO 8	DEN	47
7	CONTINUE	DEN	48
	CALL CZIEN (R,DENDZ)	DEN	49
	DEN=DENDZ*(1.000 + DEN) - REFDEN	DEN	50
	GO TO 8	DEN	51
9	CONTINUE	DEN	52
	CALL CZIEN (R,DENDZ)	DEN	53
	DEN=DENDZ*DEN	DEN	54
6	CONTINUE	DEN	55
	RETURN	DEN	56

	END	57
	SUBROUTINE ANGLE(X,Y,XLPDA)	ANG 1
	THIS SUBROUTINE COMPUTES THE ANGLE WITH THE X-AXIS FROM THE (X,Y)	ANG 2
	COORDINATES OF A POINT.	ANG 3
	NOTATION	ANG 4
	X = X-COORDINATE OF POINT	ANG 5
	Y = Y-COORDINATE OF POINT	ANG 6
	XLPDA = ANGLE WITH X-AXIS	ANG 7
	SUBROUTINES CALLED:	ANG 8
	ACNE	ANG 9
	NOTES	ANG 10
	1. XLPDA IS MEASURED IN RADIAN.	ANG 11
	2. IF X=0 AND Y=0, THEN XLPDA=0.	ANG 12
	IMPLICIT REAL*8 (A-H,O-Z)	ANG 13
	PI=3.14159265358979(0)	ANG 14
	PIDIV2=PI/2.000	ANG 15
	IF (X) 21,22,23	ANG 16
21	U=Y/X	ANG 17
	XLPDA=DATAN(U)	ANG 18
	IF (Y) 24,25,24	ANG 19
24	XLPDA=XLPDA + PI	ANG 20
	GO TO 30	ANG 21
25	XLPDA=PI	ANG 22
	GO TO 30	ANG 23
22	CONTINUE	ANG 24
	IF (Y) 27,28,29	ANG 25
27	XLPDA=-PIDIV2	ANG 26
	GO TO 30	ANG 27
28	XLPDA=0.000	ANG 28
	GO TO 30	ANG 29
29	XLPDA=PIDIV2	ANG 30
	GO TO 30	ANG 31
30	CONTINUE	ANG 32
	IF (Y) 31,32,31	ANG 33
31	U=Y/X	ANG 34
	XLPDA=DATAN(U)	ANG 35
	GO TO 30	ANG 36
32	XLPDA=0.000	ANG 37
30	CONTINUE	ANG 38
	RETURN	ANG 39
	END	ANG 40
	SUBROUTINE LGENCH(PI,NPAX)	LGE 1
	THIS SUBROUTINE COMPUTES THE NORMALIZED ASSOCIATED LEGENDRE	LGE 2
	POLYNOMIALS.	LGE 3
	NOTATION	LGE 4
	PI = GEOCENTRIC LATITUDE IN RADIAN.	LGE 5
	NPAX = MAXIMUM DEGREE AND ORDER OF THE POLYNOMIALS	LGE 6
	PRAR = ARRAY IN WHICH THE POLYNOMIALS ARE STORED	LGE 7
	SUBROUTINES CALLED:	LGE 8
	ACNE	LGE 9
	NOTES	LGE 10
	1. COMPUTES POLYNOMIALS USING KAULA'S 4*PI NORMALIZATION.	LGE 11
	2. NPAX IS LESS THAN OR EQUAL TO 180.	LGE 12
	3. DIMENSION OF PRAR IS 1 + NPAX*(NPAX+3)/2.	LGE 13
	4. POLYNOMIAL OF DEGREE N AND ORDER M IS STORED IN PRAR(INDEX),	LGE 14
	WHERE INDEX = 1 + M + N*(N+1)/2.	LGE 15
	5. SUBROUTINE HAS UNDERFLOWS WHEN PI IS NEAR THE POLES.	LGE 16
	IMPLICIT REAL*8 (A-I,C-Z)	LGE 17
	LOGICAL NOT1	LGE 18
	DIMENSION PRAR(703),SCRCOT(361)	LGE 19
	COMMON/BLKF/PRAR	LGE 20
	DATA NOT1/.FALSE./	LGE 21

	INDEXP(N)=1+P*(N+1)/2	LOG	22
	IF (ACTIST) GO TO 3	LOG	23
	NCIST=.TRUE.	LOG	24
	NCIST=2*NMAR+1	LOG	25
	IF (NSTEP-OTJ61) STOP E	LOG	26
	CC 4 I=1,NSTEP	LOG	27
4	SQRCT(1)=DSQRT(DPLCAT(1))	LOG	28
5	SINPH1=CSIN(PH1)	LOG	29
	COSPH1=CCOS(PH1)	LOG	30
	PHAR(INXP(1,0))=10C	LOG	31
	PHAR(INXP(1,1))=SQRCT(13)*SINPH1	LOG	32
	PHAR(INXP(1,1))=SQRCT(13)*COSPH1	LOG	33
	CC 2C N=2,NMAX	LOG	34
	PHAR(INXP(N,0))=SQRCT(12*N+1)/CPLD(1N)*	LOG	35
	(SQRCT(12*N+1)*SINPH1)*PHAR(INXP(N-1,0))	LOG	36
	-DPLCAT(N-1)*PHAR(INXP(N-2,0))/SQRCT(12*N-3)	LOG	37
	11=SQRCT(12*N-1)*COSPH1	LOG	38
	12=SQRCT(12)*1*PHAR(INXP(N-1,0))	LOG	39
	IF (3-N) N,P,9	LOG	40
8	T2=12+SQRCT(N-1)*SQRCT(N-2)*PHAR(INXP(N-2,1))/SQRCT(12*N-3)	LOG	41
9	PHAR(INXP(N,1))=SQRCT(12*N+1)*T2/(SQRCT(N)*SQRCT(N+1))	LOG	42
	CC 2C N=2,N	LOG	43
	T2=1*PHAR(INXP(N-1,P-1))	LOG	44
	IF (P-N+2) 11,11,12	LOG	45
11	T2=12+SQRCT(N-P)*SQRCT(N-P-1)*PHAR(INXP(N-2,M))/SQRCT(12*N-3)	LOG	46
12	PHAR(INXP(N,M))=SQRCT(12*N+1)*T2/(SQRCT(N)*SQRCT(N+1))	LOG	47
20	CONTINUE	LOG	48
	RETURN	LOG	49
	END	LOG	50
	SUBROUTINE DZENNIN,DENNZ1	DZ1	1
C			
C	THIS SUBROUTINE COMPUTES THE SPHERICALLY SYMMETRIC PART OF THE	DZ1	2
C	DENSITY DISTRIBUTION. IT USES THE AVERAGE STRUCTURE PARAMETRIZED	DZ1	3
C	EARTH MODEL OF A.P. DZIMONSKI, ET AL., "PARAMETRICALLY SIMPLE EARTH	DZ1	4
C	MODELS CONSISTENT WITH GEOPHYSICAL DATA", PHYSICS OF THE EARTH AND	DZ1	5
C	PLANETARY INTERIORS, VOLUME 10, PP. 12-40, 1975. (SEE ESPECIALLY	DZ1	6
C	TABLE 1.)	DZ1	7
C			
C	AGTATION	DZ1	8
C			
C	DENNZ1 = DENSITY IN GWAPS/CM**3	DZ1	9
C	R = RADIAL DISTANCE, NORMALIZED TO THE RADIUS OF THE EARTH	DZ1	10
C	F(J) = RADIAL DISTANCE OF DENSITY DISCONTINUITIES, ALSO	DZ1	11
C	NORMALIZED TO THE RADIUS OF THE EARTH	DZ1	12
C			
C	SUBROUTINES CALLED	DZ1	13
C			
C	NONE	DZ1	14
C			
C	IMPLICIT REAL*8(A-H,O-Z)	DZ1	15
C	DIMENSION F(11)	DZ1	16
C	COMMON/BLKN/RADAVG,RCORE,RCLOWR,NUPPER	DZ1	17
C	F(1)=0.000	DZ1	18
C	F(2)=1217.100/RADAVG	DZ1	19
C	F(3)=3485.700/RADAVG	DZ1	20
C	F(4)=5701.000/RADAVG	DZ1	21
C	F(5)=5951.000/RADAVG	DZ1	22
C	F(6)=6151.000/RADAVG	DZ1	23
C	F(7)=6291.000/RADAVG	DZ1	24
C	F(8)=6352.000/RADAVG	DZ1	25
C	F(9)=6357.000/RADAVG	DZ1	26
C	F(10)=6368.000/RADAVG	DZ1	27
C	F(11)=1.000	DZ1	28
C	IF (R - F(2)) 1,1,2	DZ1	29
C	1	DZ1	30
1	DENNZ1=13.0121900 - 8.4529200*(R**2)	DZ1	31
	GO TO 19	DZ1	32
2	CONTINUE	DZ1	33
	IF (R - F(3)) 3,3,4	DZ1	34
C	3	DZ1	35
3	DENNZ1=12.5841600 - 1.6592900*R - 1.9412800*(R**2) - 7.1121500*(R**3)	DZ1	36
	GO TO 19	DZ1	37
4	CONTINUE	DZ1	38
	IF (R - F(4)) 5,5,6	DZ1	39
C	5	DZ1	40
5	DENNZ1=6.8143000 - 1.6273300*R - 1.1853100*(R**2)	DZ1	41
	GO TO 19	DZ1	42
6	CONTINUE	DZ1	43
	IF (R - F(5)) 7,7,8	DZ1	44
C	7	DZ1	45
7	DENNZ1=11.1197800 - 7.8705400*R	DZ1	46
	GO TO 19	DZ1	47
8	CONTINUE	DZ1	48
		DZ1	49

	IF (H = F(1)) 9,9,10	021	50
C	REGION 5	021	51
9	DENCZ1=7.15855DC = 3.8559900*R	021	52
	GC TC 19	021	53
10	CONTINUE	021	54
	IF (H = F(7)) 11,11,12	021	55
C	REGION 6	021	56
11	DENCZ1=7.15855DC = 3.8559900*R	021	57
	GC TC 19	021	58
12	CONTINUE	021	59
	IF (H = F(9)) 13,13,14	021	60
C	REGION 7	021	61
13	DENCZ1=7.15855DC = 3.8559900*R	021	62
	GC TC 19	021	63
14	CONTINUE	021	64
	IF (H = F(11)) 15,15,16	021	65
C	REGION 8	021	66
15	DENCZ1=2.9020000	021	67
	GC TC 19	021	68
16	CONTINUE	021	69
	IF (H = F(13)) 17,17,18	021	70
C	REGION 9	021	71
17	DENCZ1=2.8020000	021	72
	GC TC 19	021	73
C	REGION 10	021	74
18	DENCZ1=1.0300000	021	75
19	CONTINUE	021	76
	RETURN	021	77
	END	021	78
	SUBROUTINE TOPCGR (THETA,XLPCA,H)	TOP	1
C			
C	THIS SUBROUTINE COMPUTES THE TOPOGRAPHIC HEIGHT AT A POINT ON	TOP	2
C	THE SURFACE OF THE EARTH.	TOP	3
C			
C	ACTATION	TOP	4
C			
C	THETA * COLATITUDE OF POINT IN RADIAN	TOP	5
C	XLPCA * ANGLE OF POINT WITH THE X-AXIS, LYING IN THE X-Y PLANE,	TOP	6
C	MEASURED IN RADIAN	TOP	7
C	H * TOPOGRAPHIC HEIGHT IN KILOMETERS	TOP	8
C			
C	SUBROUTINES CALLED	TOP	9
C			
C	1. LEGEND	TOP	10
C			
C	IMPLICIT REAL*8(A-H,O-Z)	TOP	11
C	DIMENSION TOPC(36,37,2)	TOP	12
C	DIMENSION PHAR(703)	TOP	13
C	COMMON/BLKG/F,P1,P12,P1DIV2,SCALE,MPHOTO,MAXSYM	TOP	14
C	COMMON/BLKP/PBAR	TOP	15
C	COMMON/BLKG/LMIN,LMAX,LLQW,LLP	TOP	16
C	COMMON/BLKH/HADAVG,PCRE,RLQWEN,RUPPER	TOP	17
C	COMMON/BLKH/TCPC	TOP	18
C	CHANGE VARIABLES FROM THETA TO PHI	TOP	19
C	PHI=PIDIV2 - THETA	TOP	20
C	COMPUTE LEGENDRE POLYNOMIALS	TOP	21
C	CALL LEGEND(PHI,LMA)	TOP	22
C	COMPUTE TOPOGRAPHIC HEIGHT IN KILOMETERS	TOP	23
	SUM=0.000	TOP	24
	DC = L*LMIN,LMAX	TOP	25
	MAX=L + 1	TOP	26
	DC = P1+1,MAX	TOP	27
	XP=P1 - 1	TOP	28
	ARG=XP*XLPCA	TOP	29
	SS=CSIN(ARG)	TOP	30
	CC=CCS(ARG)	TOP	31
	IND=P1 + L*(L+1)/2	TOP	32
	SUM=SUM + ((TOPC(L,P1,1))*CC + (TOPC(L,M1,2))*SS)*(PHAR(IND))	TOP	33
	CONTINUE	TOP	34
	H=SUM/HADAVG	TOP	35
	RETURN	TOP	36
	END	TOP	37
	SUBROUTINE CIRC(NRDESC)	CIR	1
C			
C	THIS SUBROUTINE COMPUTES THE SPACES IN WHICH THE CIRCULAR-	CIR	2
C	SHAPED MAPS START AND STOP ON A PARTICULAR LINE.	CIR	3
C			
C	ACTATION	CIR	4
C			
C	NRDESC = RADIUS OF CIRCLE, MEASURED IN HORIZONTAL SPACES	CIR	5
C	LCMH1 = ARRAY IN WHICH THE SPACE WHERE THE MAP STARTS AND STOPS	CIR	6
C	ON A PARTICULAR LINE IS STORED	CIR	7

C3=S4 + 2.000*S3*Z + 2.000*S2*Z + 2.000*S*Z*Y + T*2	CUB	34
C2=-S3*Z - 3.000*S2*Z + S2*Y - S*Z*Y	CUB	35
C1=-S3*Z - S*Z*Y	CUB	36
C0=S2*Z	CUB	37
P=C2/C3	CUB	38
Q=C1/C3	CUB	39
R=C0/C3	CUB	40
A=Q - (P**2)/3.000	CUB	41
D=(2.000*(P**3) - 9.000*P*Q + 27.000*R)/27.000	CUB	42
AP=-A/3.000	CUB	43
U=2.000*DSQRT(AP)	CUB	44
W=(3.000*Q)/(A*U)	CUB	45
WP=ESCH(1.000 - W**2)/6	CUB	46
ANG3=ATAN(WP) + PI	CUB	47
ANG=(ANG3 + FCURP1)/3.000	CUB	48
BEE=L*CCOS(ANG) - P/3.000	CUB	49
THETA=PI*DIV2 + FAC*REF*PI	CUB	50
10 CONTINUE	CUB	51
RETURN	CUB	52
END	CUB	53
SUBROUTINE QLAORCIX,Y,S,XLMCA)	QUA	1
C		
C THIS SUBROUTINE COMPUTES THE LONGITUDE OF A POINT FROM ITS		
C X-Y COORDINATES IN THE VAN DER GRINTEN PROJECTION.	QUA	2
C	QUA	3
C		
C ACTATION	QUA	4
C X = X-COORDINATE OF POINT	QUA	5
C Y = Y-COORDINATE OF POINT	QUA	6
C S = SCALE LENGTH OF MAP, EQUAL TO 180 DEGREES OF	QUA	7
C LONGITUDE MEASURED ALONG THE EQUATOR	QUA	8
C XLMCA = LONGITUDE IN RADIANS	QUA	9
C		
C SUBROUTINES CALLED:	QUA	10
C ACNE	QUA	11
C		
C NOTES	QUA	12
C 1. FOR FURTHER DETAILS SEE D.P. RUBINCAM, "INVERTING X,Y GRID	QUA	13
C COORDINATES TO OBTAIN LATITUDE AND LONGITUDE IN THE VAN DER	QUA	14
C GRINTEN PROJECTION", NASA TP 8199A, AUGUST 1980.	QUA	15
C 2. S=2*RH0 IN THE NOTATION OF THE PAPER CITED.	QUA	16
C		
C IMPLICIT REAL*RIA(H,O-Z)	QUA	17
C PI=3.1415926535897930	QUA	18
C IF (X) 2,1,2	QUA	19
1 XLMCA=0.000	QUA	20
GO TO 10	QUA	21
2 CONTINUE	QUA	22
X2=X**2	QUA	23
Y2=Y**2	QUA	24
S2=S**2	QUA	25
S4=S2*S2	QUA	26
R2=S4 + 2.000*S2*(X2 - Y2) + (X2 + Y2)**2	QUA	27
ELL=(X2 + Y2 - S2 + DSQRT(R2))/(2.000*S*X)	QUA	28
XLMCA=ELL*PI	QUA	29
10 CONTINUE	QUA	30
RETURN	QUA	31
END	QUA	32
SUBROUTINE VDG (PHI,XLMCA,RADMAP,NDEG,X,Y)	VDG	1
C		
C THIS SUBROUTINE COMPUTES THE X,Y GRID COORDINATES OF A POINT	VDG	2
C IN THE VAN DER GRINTEN PROJECTION FROM ITS LATITUDE AND LONGITUDE.	VDG	3
C		
C ACTATION	VDG	4
C PHI = LATITUDE OF POINT (IN DEGREES OR RADIANS)	VDG	5
C XLMCA = LONGITUDE OF POINT (IN DEGREES OR RADIANS)	VDG	6
C RADMAP = RADIUS OF MAP	VDG	7
C NDEG = 1 IF PHI AND XLMCA ARE IN DEGREES; 0 IF IN RADIANS	VDG	8
C X = X GRID COORDINATE	VDG	9
C Y = Y GRID COORDINATE	VDG	10
C		
C SUBROUTINES CALLED:	VDG	11
C ACNE	VDG	12
C		
C NOTES	VDG	13

C	1. THE GREENWICH MERIDIAN (XLMDA=0) RUNS DOWN THE CENTER OF	VDC	14
C	THE MAP.	VDC	15
C	2. THE ORIGIN X=0, Y=0 OF THE GRID COORDINATE SYSTEM IS LOCATED	VDC	16
C	AT THE CENTER OF THE MAP (PHI=0, XLMDA=0).	VDC	17
C	3. IF THE ABSOLUTE VALUE OF BEE OR ELL .LE. EPSLON, THEN THE	VDC	18
C	VALUE IS ASSUMED TO BE ZERO. THIS IS DONE TO AVOID INFINITIES.	VDC	19
C			
	IMPLICIT REAL*8(A-H,O-Z)	VDC	20
	PI=3.141592653589796	VDC	21
	EPSLCN=1.0D-10	VDC	22
	IF (NCEG .EQ. 1) GO TO 1	VDC	23
	ELL=XLMDA/PI	VDC	24
	BEE=PHI/PI	VDC	25
	GO TO 2	VDC	26
1	ELL=XLMDA/180.0D0	VDC	27
	BEE=PHI/180.0D0	VDC	28
2	CONTINUE	VDC	29
	B=DAES(BEE)	VDC	30
	FL=CABS(ELL)	VDC	31
	IF (FL - 1.0D0) 11,11,12	VDC	32
12	CONTINUE	VDC	33
	IF (ELL) 13,13,14	VDC	34
13	ELL=2.0D0 + ELL	VDC	35
	GO TO 15	VDC	36
14	ELL=ELL - 2.0D0	VDC	37
15	FL=CABS(ELL)	VDC	38
11	CONTINUE	VDC	39
	IF (ELL) 3,4,3	VDC	40
3	SIGNL=ELL/FL	VDC	41
	FXM=C.5D0*RADMAP*(FL - 1.0D0/FL)	VDC	42
	FXM=CABS(FXM)	VDC	43
	XM=-SIGNL*FXM	VDC	44
	R=0.5D0*RADMAP*(ELL + 1.0D0/ELL)	VDC	45
	IF (R - EPSLCN) 6,6,5	VDC	46
5	SIGNB=BEE/R	VDC	47
	B1=CSCRT(1.0D0 - 2.CDC*E)	VDC	48
	B2=CSCRT(1.0D0 + 2.CDC*E)	VDC	49
	FYJ=RADMAP*(1.0D0 - B1)*E2/(B*(B2 - B1))	VDC	50
	YJ=SIGNB*FYJ	VDC	51
	S=RADMAP*(1.0D0 + B1)*E1/(B*(B2 - B1))	VDC	52
	R2=R**2	VDC	53
	S2=S**2	VDC	54
	XPYJ=XM**2 + YJ**2	VDC	55
	RS1=R2 + S2	VDC	56
	RS2=R2 - S2	VDC	57
	RS3=4.0D0*R2*S2	VDC	58
	SQUARE=RS3 - (XPYJ - RS1)**2	VDC	59
	IF (SQUARE) 16,16,17	VDC	60
16	RADCL=0.0D0	VDC	61
	GO TO 18	VDC	62
17	RADCL=DSQRT(SQUARE)	VDC	63
18	CONTINUE	VDC	64
	X=(XM*(XMYJ - RS2) + SIGNL*FYJ*RADCL)/(2.0D0*XMYJ)	VDC	65
	Y=(YJ*(XMYJ + RS2) - SIGNB*FXM*RADCL)/(2.0D0*XMYJ)	VDC	66
	GO TO 10	VDC	67
4	X=0.0D0	VDC	68
	IF (BEE) 7,8,7	VDC	69
8	Y=0.0D0	VDC	70
	GO TO 10	VDC	71
7	Y=SIGNB*RADMAP*(1.0D0 - DSQRT(1.0D0 - 4.CDC*B**2))/(2.0D0*B)	VDC	72
	GO TO 10	VDC	73
6	Y=0.0D0	VDC	74
	X=RADMAP*ELL	VDC	75
10	CONTINUE	VDC	76
	RETURN	VDC	77
	END	VDC	78

2531 CARDS